

ON MAXIMAL GREEN SEQUENCES FOR TYPE \mathbb{A} QUIVERS

ALEXANDER GARVER AND GREGG MUSIKER

ABSTRACT. Given a framed quiver, i.e. one with a frozen vertex associated to each mutable vertex, there is a concept of *green mutation*, as introduced by Keller. Maximal sequences of such mutations, known as *maximal green sequences*, are important in representation theory and physics as they have numerous applications, including the computations of spectrums of BPS states, Donaldson-Thomas invariants, tilting of hearts in derived categories, and quantum dilogarithm identities. In this paper, we study such sequences and construct a maximal green sequence for every quiver mutation-equivalent to an orientation of a type \mathbb{A} Dynkin diagram.

CONTENTS

1. Introduction	1
2. Preliminaries and Notation	3
3. Direct Sums of Quivers	4
4. Quivers Arising from Triangulated Surfaces	9
5. Signed Irreducible Type \mathbb{A} Quivers	11
6. Associated Mutation Sequences	14
6.1. Definition of Associated Mutation Sequences	14
7. Proof of Theorem 6.5	19
8. Additional Questions and Remarks	28
8.1. Maximal Green Sequences for Quivers Arising from Surface Triangulations	28
8.2. Trees of Cycles	33
8.3. Enumeration of Maximal Green Sequences	33
8.4. Further Study of Maximal Green Sequences	34
References	34

1. INTRODUCTION

A very important problem in cluster algebra theory, with connections to polyhedral combinatorics and the enumeration of BPS states in string theory, is to determine when a given quiver has a maximal green sequence. In particular, it is open to decide which quivers arising from triangulations of surfaces admit a maximal green sequence, although progress for surfaces has been made in [17], [7], [8] and in the physics literature in [1]. In [1], they give heuristics for exhibiting maximal green sequences for quivers arising from triangulations of surfaces with boundary and present examples of this for spheres with at least 4 punctures and tori with at least 2 punctures. They write down a particular triangulation of such a surface and show that the quiver defined by this triangulation has a maximal green sequence. In [7, 8], this same approach is used on surfaces of any genus with at least 2 punctures. In [17], it is shown that there do not exist maximal green sequences for a quiver arising from any triangulation of a closed once-punctured genus g surface. It is still unknown the exact set of surfaces with the property that each of its triangulations defines a quiver admitting a maximal green sequence.

Outside the class of quivers defined by triangulated surfaces there has also been progress in proving that certain quivers do not have maximal green sequences. In [5], it is shown that if a quiver has non-degenerate Jacobi-infinite potential, then the quiver has no maximal green sequences. This is used in [5] to show that a certain McKay quiver has no maximal green sequences, and in [22] it is shown that the \mathbb{X}_7 quiver has no maximal green sequences. Other work [18] illustrates that it is possible to have two mutation-infinite quivers that are mutation equivalent to one another where only one of the two admits a maximal green sequence.

Even for cases where the existence of maximal green sequences is known (e.g. for *quivers of type \mathbb{A}*), the problem of exhibiting, classifying or counting maximal green sequences has been challenging and serves as our motivation. By a quiver of type \mathbb{A} , we mean any quiver that is *mutation-equivalent* to an orientation of a type

A Dynkin diagram. In the case where Q is acyclic, one can find a maximal green sequence whose length is the number of vertices of Q , by mutating at sources and iterating until all vertices have been mutated exactly once. In general, maximal green sequences must have length at least the number of vertices of Q . However, even for the smallest non-acyclic quiver, i.e. the oriented 3-cycle (of type A_3), a shortest maximal green sequence is of length 4. (While we were in the process of revising this paper, it was shown in [9] that the shortest possible length of a maximal green sequence for a quiver Q of type A_n is $n + t$ where $t = \#\{3\text{-cycles of } Q\}$. See Remark 6.7 and Sections 8.1 and 8.3 for more details.) With a goal of gaining a better understanding of such sequences, in this paper we *explicitly* construct a maximal green sequence for every quiver of type A . As any triangulation of the disk with $n + 3$ marked points on the boundary defines a quiver of type A_n , our construction shows that the disk belongs to the set of surfaces each of whose triangulations define a quiver admitting a maximal green sequence. We remark that the latter result has also been proved in [9] by constructing maximal green sequences of type A_n quivers of shortest possible length. Additionally, the maximal green sequences constructed in [9] are almost never the same as the maximal green sequences constructed in this paper.

In Section 2, we begin with background on quivers and their mutations. This section includes the definition of *maximal green sequences*, which is our principal object of study in this paper. Section 3 describes how to decompose quivers into *direct sums* of strongly connected components, which we call irreducible quivers. We remark that this definition of direct sum of quivers, which is based on a quiver gluing rule from [1], coincides with the definition of a triangular extension of quivers appearing in [2]. Using this notion of direct sums in Theorem 3.12, we show that for certain direct sums of quivers, to construct a maximal green sequence, it suffices to construct a maximal green sequence for each of their irreducible components. We refer to the class of such quivers for which Theorem 3.12 holds as *t-colored direct sums* of quivers (see Definition 3.1). In Section 4, we show that almost all quivers arising from triangulated surfaces (with 1 connected component) which are a direct sum of at least 2 irreducible components are in fact a *t-colored directed sum*.

For type A quivers, irreducible quivers have an especially nice form as trees of 3-cycles, as described by Corollary 5.2. This allows us to restrict our attention to *signed irreducible* quivers of type A , which are defined in and studied in Section 5. We then construct a special mutation sequence for every signed irreducible quiver of type A in Section 6, which we call an *associated mutation sequence*. This brings us to the main theorem of the paper, Theorem 6.5, which states that this associated mutation sequence is a maximal green sequence. Section 6 also highlights how the results of Section 3 can be combined with Theorem 6.5 to get maximal green sequences for *any* quiver of type A (see Corollary 6.8).

The proof of Theorem 6.5 is somewhat involved. The proof of Theorem 6.5 essentially follows from two important lemmas (see Lemma 7.2 and Lemma 7.3). Our proof begins by attaching *frozen vertices* to a signed irreducible type A quiver Q to get a *framed quiver* \hat{Q} (see Section 2 for more details). We then apply the associated mutation sequence $\underline{\mu}$ alluded to above, which is constructed in Section 6, but decompose it into certain subsequences as $\underline{\mu} = \underline{\mu}_n \circ \cdots \circ \underline{\mu}_1 \circ \underline{\mu}_0$ and apply each mutation subsequence $\underline{\mu}_k$ one after the other. In Lemma 7.2 we explicitly describe, for the resulting intermediate quivers, the full subquiver that will be affected by the next iteration of mutations $\underline{\mu}_k$. We will refer to this full subquiver of $\underline{\mu}_{k-1} \circ \cdots \circ \underline{\mu}_1 \circ \underline{\mu}_0(\hat{Q})$ affected by $\underline{\mu}_k$ as \bar{R}_k . Lemma 7.3 then explicitly describes how each of these full subquivers, \bar{R}_k , is affected by the mutation sequence $\underline{\mu}_k$. Together these lemmas lead us to conclude that the associated mutation sequence $\underline{\mu} = \underline{\mu}_n \circ \cdots \circ \underline{\mu}_1 \circ \underline{\mu}_0$ is a maximal green sequence.

Furthermore, these two lemmas imply that the final quiver $\underline{\mu}_n \circ \cdots \circ \underline{\mu}_1 \circ \underline{\mu}_0(\hat{Q})$ is isomorphic (as a directed graph) to \check{Q} , the *co-framed* quiver where the directions of arrows between vertices of Q and frozen vertices have all been reversed. In particular, such an isomorphism is known as a *frozen isomorphism* since it permutes the vertices of Q while leaving the frozen vertices fixed. We refer to this permutation, of vertices of Q , as the *permutation induced* by a maximal green sequence (we refer the reader to Section 2 for precise definitions of these notions). One of the benefits of proving Theorem 6.5 using the two lemmas mentioned in the previous paragraph is that we exactly describe the permutation that is induced by an associated mutation sequence of a signed irreducible quiver of type A . (See the last paragraph in Section 2 and Definition 7.1.) This is a result that may be of independent interest.

Finally, Section 8 ends with further remarks and ideas for future directions, including extensions to quivers arising from triangulations of surfaces other than the disk with marked points on the boundary.

Acknowledgements. The authors would like to thank T. Brüstle, M. Del Zotto, B. Keller, S. Ladkani, R. Patrias, V. Reiner, and H. Thomas for useful discussions. We also thank the referees for their careful reading

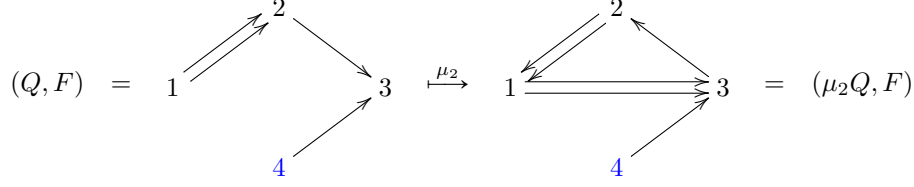


FIGURE 1. An example of quiver mutation.

and numerous suggestions. The authors were supported by NSF Grants DMS-1067183, DMS-1148634, and DMS-1362980.

2. PRELIMINARIES AND NOTATION

The reader may find excellent surveys on the theory of cluster algebras and maximal green sequences in [5, 14]. For our purposes, we recall a few of the relevant definitions.

A **quiver** Q is a directed graph without loops or 2-cycles. In other words, Q is a 4-tuple $((Q)_0, (Q)_1, s, t)$, where $(Q)_0 = [M] := \{1, 2, \dots, M\}$ is a set of **vertices**, $(Q)_1$ is a set of **arrows**, and two functions $s, t : (Q)_1 \rightarrow (Q)_0$ are defined so that for every $\alpha \in (Q)_1$, we have $s(\alpha) \xrightarrow{\alpha} t(\alpha)$. An **ice quiver** is a pair (Q, F) with Q a quiver and $F \subset (Q)_0$ **frozen vertices** with the additional restriction that any $i, j \in F$ have no arrows of Q connecting them. We refer to the elements of $(Q)_0 \setminus F$ as **mutable vertices**. By convention, we assume $(Q)_0 \setminus F = [N]$ and $F = [N + 1, M] := \{N + 1, N + 2, \dots, M\}$. Any quiver Q can be regarded as an ice quiver by setting $Q = (Q, \emptyset)$.

The **mutation** of an ice quiver (Q, F) at a mutable vertex k , denoted μ_k , produces a new ice quiver $(\mu_k Q, F)$ by the three step process:

- (1) For every 2-path $i \rightarrow k \rightarrow j$ in Q , adjoin a new arrow $i \rightarrow j$.
- (2) Reverse the direction of all arrows incident to k in Q .
- (3) Delete any 2-cycles created during the first two steps.

We show an example of mutation in Figure 1 depicting the mutable (resp. frozen) vertices in black (resp. blue). Since we will focus on quiver mutation in this paper, it will be useful to define a notation for arrows obtained by reversing their direction. Given $\alpha \in (Q)_1$ where $s(\alpha) \xrightarrow{\alpha} t(\alpha)$, formally define α^{op} to be the arrow where $s(\alpha^{\text{op}}) = t(\alpha)$ and $t(\alpha^{\text{op}}) = s(\alpha)$. With this notation, step (2) in the definition of mutation can be rephrased as: if $\alpha \in (Q)_1$ and $s(\alpha) = k$ or $t(\alpha) = k$, replace α with α^{op} .

The information of an ice quiver can be equivalently described by its (skew-symmetric) **exchange matrix**. Given (Q, F) , we define $B = B_{(Q, F)} = (b_{ij}) \in \mathbb{Z}^{N \times M} := \{N \times M \text{ integer matrices}\}$ by $b_{ij} := \#\{(i \xrightarrow{\alpha} j) \in (Q)_1\} - \#\{(j \xrightarrow{\alpha} i) \in (Q)_1\}$. Furthermore, ice quiver mutation can equivalently be defined as **matrix mutation** of the corresponding exchange matrix. Given an exchange matrix $B \in \mathbb{Z}^{N \times M}$, the **mutation** of B at $k \in [N]$, also denoted μ_k , produces a new exchange matrix $\mu_k(B) = (b'_{ij})$ with entries

$$b'_{ij} := \begin{cases} -b_{ij} & : \text{ if } i = k \text{ or } j = k \\ b_{ij} + \text{sgn}(b_{ik})[b_{ik}b_{kj}]_+ & : \text{ otherwise} \end{cases}$$

where $[x]_+ = \max(x, 0)$. For example, the mutation of the ice quiver above (here $M = 4$ and $N = 3$) translates into the following matrix mutation. Note that mutation of matrices (or of ice quivers) is an involution (i.e. $(\mu_k \circ \mu_k)(B) = B$).

$$B_{(Q, F)} = \left[\begin{array}{ccc|c} 0 & 2 & 0 & 0 \\ -2 & 0 & 1 & 0 \\ 0 & -1 & 0 & -1 \end{array} \right] \xrightarrow{\mu_2} \left[\begin{array}{ccc|c} 0 & -2 & 2 & 0 \\ 2 & 0 & -1 & 0 \\ -2 & 1 & 0 & -1 \end{array} \right] = B_{(\mu_2 Q, F)}.$$

In this paper, we focus on successively applying mutations to a fixed ice quiver. As such, if (Q, F) is a given ice quiver we define an **admissible sequence** of (Q, F) , denoted $\mathbf{i} = (i_1, \dots, i_d)$, to be a sequence of mutable vertices of (Q, F) such that $i_j \neq i_{j+1}$ for all $j \in [d - 1]$. An admissible sequence $\mathbf{i} = (i_1, \dots, i_d)$ also gives rise to a **mutation sequence**, which we define to be an expression $\underline{\mu} = \mu_{i_d} \circ \dots \circ \mu_{i_1}$ with $i_j \neq i_{j+1}$ for all $j \in [d - 1]$ that maps an ice quiver (Q, F) to a mutation-equivalent one¹. Let $\text{Mut}((Q, F))$ denote the collection of ice quivers obtainable from (Q, F) by a mutation sequence of **finite length** where the **length** of a mutation sequence is defined to be d , the number of vertices appearing in the associated admissible sequence $\mathbf{i} = (i_1, \dots, i_d)$. Given

¹In the sequel, we will identify an admissible sequence with the mutation sequence it defines.

a mutation sequence $\underline{\nu}$ of $\bar{Q} \in \text{Mut}(\hat{Q})$ we define the **support** of $\underline{\nu}$, denoted $\text{supp}(\underline{\nu})$, to be the set of mutable vertices of \bar{Q} appearing in the admissible sequence which gives rise to $\underline{\nu}$.

Given a quiver Q , we focus on successively mutating the framed quiver of Q , which we now define. Following references such as [5, Section 2.3], given a quiver Q , we define its **framed** (resp. **coframed**) quiver to be the ice quiver \hat{Q} (resp. \check{Q}) where $(\hat{Q})_0 = (\check{Q})_0 := (Q)_0 \sqcup [N+1, 2N]$, $F = [N+1, 2N]$, and $(\hat{Q})_1 := (Q)_1 \sqcup \{i \rightarrow N+i : i \in [N]\}$ (resp. $(\check{Q})_1 := (Q)_1 \sqcup \{N+i \rightarrow i : i \in [N]\}$). We will denote elements of $\text{Mut}(\hat{Q})$ by \bar{Q} . In the sequel, we will often write frozen vertices $N+i$ of $\bar{Q} \in \text{Mut}(\hat{Q})$ as i' . Thus $F = [N]'$ where $S' := \{x' : x \in S\}$ for any $S \subset (Q)_0$. In this paper, we consider ice quivers $\bar{Q} \in \text{Mut}(\hat{Q})$ up to **frozen isomorphism** (i.e. an isomorphism of quivers that fixes frozen vertices). Such an isomorphism is equivalent to a simultaneous permutation of the rows and of the first N columns of the exchange matrix $B_{\bar{Q}}$.

A mutable vertex i of an ice quiver $\bar{Q} \in \text{Mut}(\hat{Q})$ is said to be **green** (resp. **red**) if all arrows of \bar{Q} connecting an element of $[N]'$ and i point away from (resp. towards) i . Note that all mutable vertices of \hat{Q} are green and all vertices of \check{Q} are red. By the Sign-Coherence of **c**- and **g**-vectors for cluster algebras [10, Theorem 1.7], it follows that given any $\bar{Q} \in \text{Mut}(\hat{Q})$ each mutable vertex of \bar{Q} is either red or green.

Let $\underline{\mu} = \mu_{i_d} \circ \dots \circ \mu_{i_1}$ be a mutation sequence of \hat{Q} . Define $\{\bar{Q}(k)\}_{0 \leq k \leq d}$ to be the sequence of ice quivers where $\bar{Q}(0) := \hat{Q}$ and $\bar{Q}(j) := (\mu_{i_j} \circ \dots \circ \mu_{i_1})(\hat{Q})$. (In particular, throughout this paper, we apply any sequence of mutations in order from right-to-left.) A **green sequence** of Q is an admissible sequence $\mathbf{i} = (i_1, i_2, \dots, i_d)$ of \hat{Q} such that i_j is a green vertex of $\bar{Q}(j-1)$ for each $1 \leq j \leq d$. The admissible sequence \mathbf{i} is a **maximal green sequence** of Q if it is a green sequence of Q such that in the final quiver $\bar{Q}(d)$, the vertices $1, 2, \dots, N$ are all red². In other words, $\bar{Q}(d)$ contains no green vertices. Following [5], we let $\text{green}(Q)$ denote the set of maximal green sequences of Q ³.

Proposition 2.10 of [5] shows that given any maximal green sequence $\underline{\mu}$ of Q , one has a frozen isomorphism $\bar{Q}(d) \cong \check{Q}$. Such an isomorphism amounts to a permutation of the mutable vertices of \check{Q} , (i.e. $\bar{Q}(d) = \check{Q}\sigma$ for some permutation $\sigma \in \mathfrak{S}_N$ where $\check{Q}\sigma$ is defined by the exchange matrix $B\sigma = B_{\check{Q}}\sigma$ that has entries $(B\sigma)_{i,j} = B_{i\cdot\sigma, j\cdot\sigma}$). We call this the **permutation induced** by $\underline{\mu}$. Note that we can regard σ as an element \mathfrak{S}_{2N} where $i \cdot \sigma = i$ for any $i \in [N+1, 2N]$.

3. DIRECT SUMS OF QUIVERS

In this section, we define a direct sum of quivers based on notation appearing in [1, Section 4.2]. We also show that, under certain restrictions, if a quiver Q can be written as a direct sum of quivers where each summand has a maximal green sequence, then the maximal green sequences of the summands can be concatenated in some way to give a maximal green sequence for Q . Throughout this section, we let (Q_1, F_1) and (Q_2, F_2) be finite ice quivers with N_1 and N_2 vertices, respectively. Furthermore, we assume $(Q_1)_0 \setminus F_1 = [N_1]$ and $(Q_2)_0 \setminus F_2 = [N_1+1, N_1+N_2]$.

Definition 3.1. Let (a_1, \dots, a_k) denote a k -tuple of elements from $(Q_1)_0 \setminus F_1$ and (b_1, \dots, b_k) a k -tuple of elements from $(Q_2)_0 \setminus F_2$. (By convention, we assume that the k -tuple (a_1, \dots, a_k) is ordered so that $a_i \leq a_j$ if $i < j$ unless stated otherwise.) Additionally, let $(R_1, F_1) \in \text{Mut}((Q_1, F_1))$ and $(R_2, F_2) \in \text{Mut}((Q_2, F_2))$. We define the **direct sum** of (R_1, F_1) and (R_2, F_2) , denoted $(R_1, F_1) \oplus_{(a_1, \dots, a_k)}^{(b_1, \dots, b_k)} (R_2, F_2)$, to be the ice quiver with vertices

$$\left((R_1, F_1) \oplus_{(a_1, \dots, a_k)}^{(b_1, \dots, b_k)} (R_2, F_2) \right)_0 := (R_1)_0 \sqcup (R_2)_0 = (Q_1)_0 \sqcup (Q_2)_0 = [N_1 + N_2] \sqcup F_1 \sqcup F_2$$

and arrows

$$\left((R_1, F_1) \oplus_{(a_1, \dots, a_k)}^{(b_1, \dots, b_k)} (R_2, F_2) \right)_1 := (R_1, F_1)_1 \sqcup (R_2, F_2)_1 \sqcup \left\{ a_i \xrightarrow{\alpha_i} b_i : i \in [k] \right\}.$$

Observe that we have the identification of ice quivers

$$Q_1 \oplus_{(a_1, \dots, a_k)}^{(b_1, \dots, b_k)} Q_2 \cong \widehat{Q}_1 \oplus_{(a_1, \dots, a_k)}^{(b_1, \dots, b_k)} \widehat{Q}_2,$$

where the total number of vertices $M = 2(N_1 + N_2)$ in both cases.

²Note that since we identify an admissible sequence with the mutation sequence defined by it, we have that maximal green sequences are identified with maximal green mutation sequences, as they are referred to in [19].

³By identifying maximal green sequences with maximal green mutation sequences, we abuse notation and write an element of $\text{green}(Q)$ either as an admissible sequence $\mathbf{i} = (i_1, \dots, i_d)$ or as its corresponding mutation sequence $\underline{\mu} = \mu_{i_d} \circ \dots \circ \mu_{i_1}$.

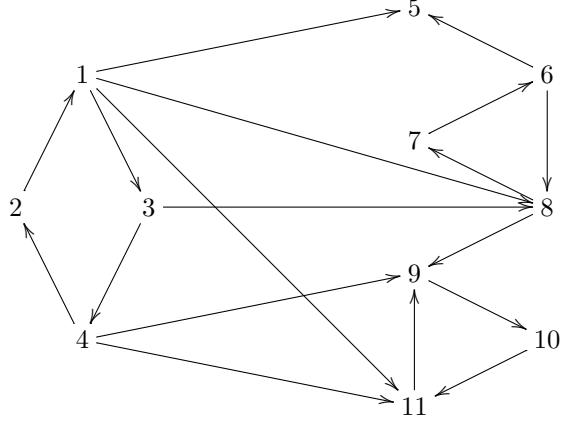


FIGURE 2. The quiver Q used in Example 3.5.

We say that $(R_1, F_1) \oplus_{(a_1, \dots, a_k)}^{(b_1, \dots, b_k)} (R_2, F_2)$ is a **t -colored direct sum** if $t = \#\{\text{distinct elements of } \{a_1 \dots, a_k\}\}$ and there does not exist i and j such that

$$\# \{a_i \xrightarrow{\alpha} b_j\} \geq 2.$$

Remark 3.2. Our definition of the direct sum of two quivers coincides with the definition of a **triangular extension** of two quivers introduced by C. Amiot in [2], except that we consider quivers as opposed to quivers with potential. We thank S. Ladkani for bringing this to our attention. He uses this terminology to study the representation theory of a related class of quivers with potential, called class \mathcal{P} by M. Kontsevich and Y. Soibelman [16, Section 8.4].

Remark 3.3. The direct sum of two ice quivers is a non-associative operation as is shown in Example 3.5.

Definition 3.4. We say that a quiver Q is **irreducible** if

$$Q = Q_1 \oplus_{(a_1, \dots, a_k)}^{(b_1, \dots, b_k)} Q_2$$

for some k -tuple $(a_1 \dots, a_k)$ on $(Q_1)_0$ and some k -tuple (b_1, \dots, b_k) on $(Q_2)_0$ implies that Q_1 or Q_2 is the empty quiver. Note that we define irreducibility only for quivers rather than for ice quivers because we later only study reducibility when $F = \emptyset$.

Example 3.5. Let Q denote the quiver shown in Figure 2. Define Q_1 to be the full subquiver of Q on the vertices $1, \dots, 4$, Q_2 to be the full subquiver of Q on the vertices $6, \dots, 11$, and Q_3 to be the full subquiver of Q on the vertex 5. Note that Q_1, Q_2 , and Q_3 are each irreducible. Then

$$Q = Q_1 \oplus_{(1,1,1,3,4,4)}^{(5,8,11,8,9,11)} Q_{23}$$

where $Q_{23} = Q_2 \oplus_{(6)}^{(5)} Q_3$ so Q is a 3-colored direct sum. On the other hand, we could write

$$Q = Q_{12} \oplus_{(1,6)}^{(5,5)} Q_3$$

where $Q_{12} = Q_1 \oplus_{(1,1,3,4,4)}^{(8,11,8,9,11)} Q_2$ so Q is a 2-colored direct sum. Additionally, note that

$$Q_1 \oplus_{(1,1,1,3,4,4)}^{(5,8,11,8,9,11)} Q_{23} = Q_1 \oplus_{(1,1,1,3,4,4)}^{(5,8,11,8,9,11)} \left(Q_2 \oplus_{(6)}^{(5)} Q_3 \right) \neq \left(Q_1 \oplus_{(1,1,1,3,4,4)}^{(5,8,11,8,9,11)} Q_2 \right) \oplus_{(6)}^{(5)} Q_3$$

where the last equality does not hold because $Q_1 \oplus_{(1,1,1,3,4,4)}^{(5,8,11,8,9,11)} Q_2$ is not defined as 5 is not a vertex of Q_2 . This shows that the direct sum of two quivers, in the sense of this paper, is not associative.

Our next goal is to prove that Q has a maximal green sequence if Q is a t -colored direct sum and each of its summands has a maximal green sequence (see Proposition 3.12). Before proving this, we introduce a standard form of t -colored direct sums of ice quivers with which we will work:

$$(1) \quad (R, F) = \widehat{Q}_1 \oplus_{(a_1, \dots, a_1, \dots, a_t, \dots, a_t)}^{(b_1^{(1)}, \dots, b_{r_1}^{(1)}, \dots, b_1^{(t)}, \dots, b_{r_t}^{(t)})} \overline{Q}_2$$

where $\overline{Q}_2 \in \text{Mut}(\widehat{Q}_2)$, $a_1, \dots, a_t \in (Q_1)_0 \setminus [N_1]'$, $b_1^{(1)}, \dots, b_{r_1}^{(1)}, \dots, b_1^{(t)}, \dots, b_{r_t}^{(t)} \in (Q_2)_0 \setminus [N_2]'$, and $\underline{\mu}$ is a fixed mutation sequence $\mu_{i_d} \circ \dots \circ \mu_{i_1}$ where $\text{supp}(\underline{\mu}) \subset (Q_1)_0$.

We consider the sequence of mutated quivers $(R^{(k)}, F)$, for each $k \in [0, d]$, where $R^{(k)} := \mu_{i_k} \circ \dots \circ \mu_{i_1} R$. By convention, $k = 0$ implies that the empty mutation sequence has been applied to (R, F) so $R^{(0)} = R$. For every $k \in [0, d]$, we define $\overline{Q}_1(k) := (\mu_{i_k} \circ \dots \circ \mu_{i_1})(\widehat{Q}_1)$ and the following set of arrows

$$A(k) := \left\{ \alpha \in (R^{(k)}, F)_1 : \begin{array}{l} s(\alpha) \text{ or } t(\alpha) \in (\overline{Q}_1(k))_0 \setminus [N_1]' \text{ and the other end of } \\ \alpha \text{ is in } \{a'_1, \dots, a'_t\} \cup \{b_1^{(1)}, \dots, b_{r_1}^{(1)}, \dots, b_1^{(t)}, \dots, b_{r_t}^{(t)}\} \end{array} \right\}.$$

Observe that the sets $A(k)$ only contain arrows in the partially mutated quivers which have exactly one of their two ends incident to a vertex in $(Q_1)_0$. The next lemma illustrates how the set of arrows $A(k-1)$ transforms into the set $A(k)$.

Lemma 3.6. If $(i \xrightarrow{\alpha} j) \in A(k)$, but $\alpha, \alpha^{\text{op}} \notin A(k-1)$, then there is a 2-path $i \xrightarrow{\alpha_1} i_k \xrightarrow{\alpha_2} j$ in $(R^{(k-1)}, F)$ and exactly one of the arrows $\alpha_1, \alpha_2 \in (R^{(k-1)}, F)_1$ belongs to $A(k-1)$.

Proof. By the definition of quiver mutation, the arrow $(i \xrightarrow{\alpha} j) \in A(k) \subset (R^{(k)}, F)_1 = (\mu_{i_k} R^{(k-1)}, F)_1$ was originally in $A(k-1)$, was the reversal of an arrow originally in $A(k-1)$, or resulted from a 2-path.

By hypothesis, we must be in the last case. By the definition of $A(k)$, either the source or target of α is in $(\overline{Q}_1(k))_0 \setminus [N_1]'$ but not both. Hence the 2-path $i \xrightarrow{\alpha_1} i_k \xrightarrow{\alpha_2} j$ must contain one arrow from $(\overline{Q}_1(k))_0 \setminus [N_1]'$ to itself and one arrow in $A(k-1)$. \square

In the context of this lemma, we refer to this unique arrow in $A(k-1)$ as $\overline{\alpha}$. We use Lemma 3.6 to define a **coloring function** to stratify the set of arrows $A(k)$. This will allow us to keep track of their orientations as will be needed to prove a crucial lemma (see Lemma 3.10).

Definition 3.7. Let (R, F) be a t -colored direct sum with a direct sum decomposition of the form shown in (1) and let $\underline{\mu}$ be a mutation sequence where $\text{supp}(\underline{\mu}) \subset (Q_1)_0$. Define a **coloring function** by

$$\begin{aligned} f^0 : A(0) &\longrightarrow \{a_1, \dots, a_t\} \\ \alpha &\longmapsto s(\alpha). \end{aligned}$$

We say that $\alpha \in A(0)$ has **color** $f^0(\alpha)$ in (R, F) . Now, inductively we define a coloring function on each ice quiver $(R^{(k)}, F)$ where $k \in [0, d]$. Define $f^k : A(k) \rightarrow \{a_1, \dots, a_t\}$ by

$$f^k(\alpha) = \begin{cases} f^{k-1}(\overline{\alpha}) & : \text{ if } \alpha, \alpha^{\text{op}} \notin A(k-1) \\ f^{k-1}(\alpha^{\text{op}}) & : \text{ if } \alpha \notin A(k-1), \alpha^{\text{op}} \in A(k-1), \\ f^{k-1}(\alpha) & : \text{ if } \alpha \in A(k-1). \end{cases}$$

We say that $\alpha \in A(k)$ has **color** $f^k(\alpha)$ in $(R^{(k)}, F)$.

Example 3.8. Using the notation from Example 3.5 and writing

$$\widehat{Q} = \widehat{Q}_1 \oplus_{(1,1,1,3,4,4)}^{(5,8,11,8,9,11)} \left(\widehat{Q}_2 \oplus_{(6)}^{(5)} \widehat{Q}_3 \right),$$

we have $a_1 = 1$ and $b_1^{(1)} = 5, b_2^{(1)} = 8, b_3^{(1)} = 11, a_2 = 3$ and $b_1^{(2)} = 8$, and $a_3 = 4$ and $b_1^{(3)} = 9, b_2^{(3)} = 11$. In Figure 3, we show \widehat{Q} and $\mu_3 \widehat{Q}$. The label written on an arrow α of \widehat{Q} or $\mu_3 \widehat{Q}$ indicates its color with respect to Q_1 .

Our next result shows how the coloring functions $\{f^k\}_{0 \leq k \leq d}$ defined by an ice quiver (R, F) of the form in (1) and a mutation sequence $\underline{\mu} = \mu_{i_d} \circ \dots \circ \mu_{i_1}$ partition the arrows connecting a mutable vertex $x \in (Q_1)_0$ and a vertex in $\{b_i^{(j)} : i \in [r_j]\} \sqcup \{a'_j\}$.

Lemma 3.9. Let (R, F) be a t -colored direct sum with a direct sum decomposition of the form shown in (1) and let $\underline{\mu}$ be a mutation sequence where $\text{supp}(\underline{\mu}) \subset (Q_1)_0$. For any $k \in [0, d]$, we have that the coloring function f^k is defined on each $\alpha \in A(k)$.

Proof. We proceed by induction on k . If $k = 0$, no mutations have been applied so the desired result holds. Suppose the result holds for $(R^{(k-1)}, F)$ and we will show that the result also holds for $(R^{(k)}, F)$. We can write $(R^{(k)}, F) = (\mu_y R^{(k-1)}, F)$ for some $y \in (Q_1)_0$. Let $\alpha \in A(k)$ such that $s(\alpha) = x \in (Q_1)_0$ and $t(\alpha) = z \in \{b_i^{(j)} : i \in [r_j]\} \sqcup \{a'_j\}$ or vice-versa. There are three cases to consider:

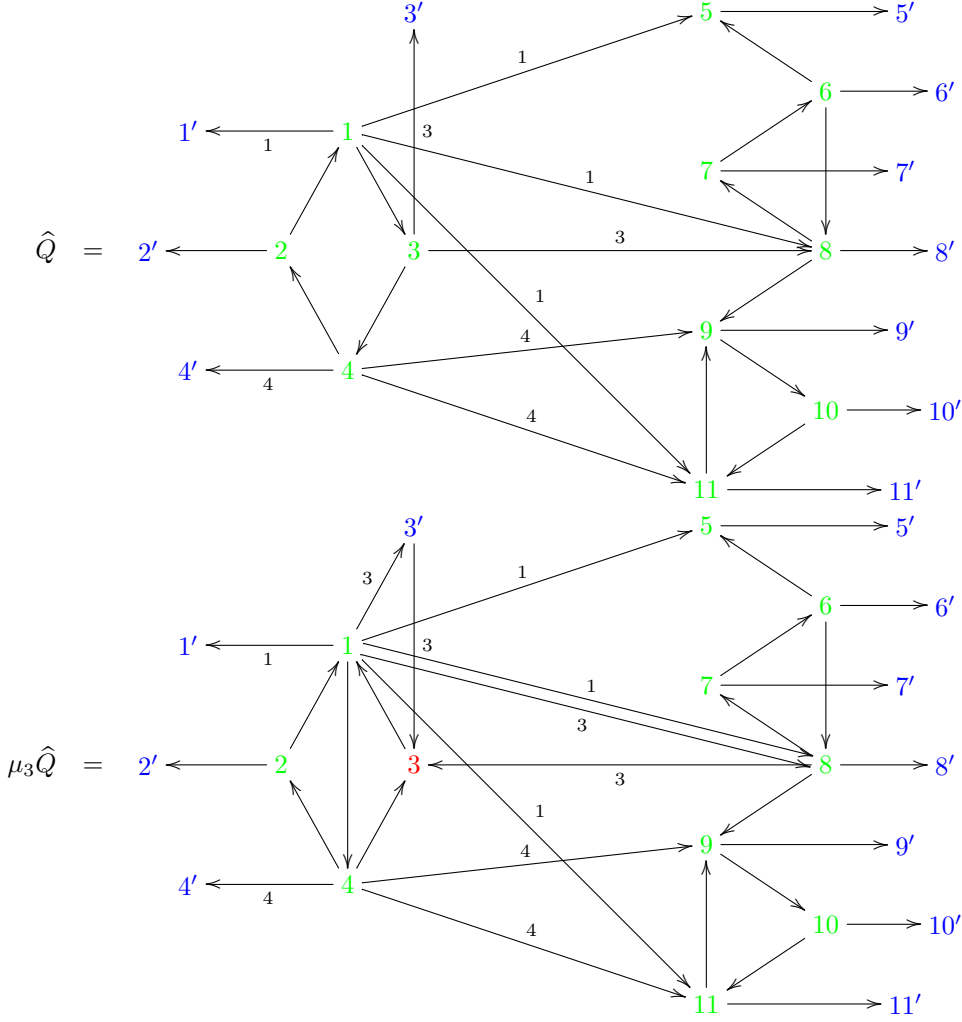


FIGURE 3. The quivers \hat{Q} and $\mu_3 \hat{Q}$ with the coloring functions f^1 and f^2 , respectively.

- a) $x = y$,
- b) x is connected to y and there is a 2-path $x \rightarrow y \rightarrow z$ or $x \leftarrow y \leftarrow z$ in $(R^{(k-1)}, F)$,
- c) x does not satisfy a) or b).

In *Case a)*, we have that all arrows $\alpha \in A(k-1)$ connecting x and z are replaced by $\alpha^{\text{op}} \in A(k)$. By the definition of the coloring functions, these reversed arrows obtain color $f^k(\alpha) = f^{k-1}(\alpha^{\text{op}})$.

In *Case b)*, it follows by Lemma 3.6 that an arrow $\alpha \in A(k)$ resulting from mutation of the middle of a 2-path has a well-defined color given by $f^{k-1}(\bar{\alpha})$. Further, mutation at y would reverse both arrows of such a 2-path hence vertex y is in the middle of a 2-path in $A(k)$ if and only if it is in the middle of a 2-path in $A(k-1)$.

Finally, in *Case c)*, the mutation at y does not affect the arrows α connecting x and z and therefore the colors of such an arrow is inherited from its color as an arrow in $A(k-1)$. Note that an arrow between x and y would connect vertices of $(Q_1)_0$ and thus has no color. \square

For the proofs in the remainder of this section, we denote the exchange matrix of $(R^{(k)}, F)$, as $B_{(R^{(k)}, F)} = (b^k(x, y))_{x \in [N_1 + N_2], y \in [2(N_1 + N_2)]}$. Here $b^k(x, y) := \#\{(x \xrightarrow{\alpha} y) \in (R^{(k)}, F)_1\} - \#\{(y \xrightarrow{\alpha} x) \in (R^{(k)}, F)_1\}$. (This differs from the notation of Section 2 to differentiate it from our notation for the set of vertices $\{b_i^{(j)} : i \in [r_j]\}$.) Furthermore, we refine this enumeration according to color using the following terminology.

$$b^k(x, y, \ell) := \#\{(x \xrightarrow{\alpha} y) \in (R^{(k)}, F)_1 : \alpha \text{ has color } \ell\} - \#\{(y \xrightarrow{\alpha} x) \in (R^{(k)}, F)_1 : \alpha \text{ has color } \ell\}.$$

We proceed with the following two technical lemmas.

Lemma 3.10. Let (R, F) be a t -colored direct sum with a direct sum decomposition of the form shown in (1) and let $\underline{\mu}$ be a mutation sequence of (R, F) where $\text{supp}(\underline{\mu}) \subset (Q_1)_0$. For any $k \in [0, d]$, $\ell \in [t]$, and $x \in (Q_1)_0$, all of the arrows of $A(k)$ with color a_ℓ and incident to vertex x either all point towards vertex x or all point away from vertex x . Moreover they do so with the same multiplicity.

Proof. We need to show that for any $x \in (Q_1)_0$, $k \in [0, d]$, $j \in [t]$, and $\ell \in \{a_1, \dots, a_t\}$ we have that $b^k(x, b_i^{(j)}, \ell) = b^k(x, a'_j, \ell)$ for all $i \in [r_j]$. We proceed by induction on k . If $k = 0$, no mutations have been applied so the desired results holds. Suppose the result holds for $(R^{(k-1)}, F)$ and we will show that the result also holds for $(R^{(k)}, F)$. We can write $(R^{(k)}, F) = (\mu_y R^{(k-1)}, F)$ for some $y \in (Q_1)_0$. Let $x \in (Q_1)_0$ and $z \in \{b_i^{(j)} : i \in [r_j]\} \sqcup \{a'_j\}$ be given. There are three cases to consider:

- a) $x = y$,
- b) x is connected to y and $\text{sgn}(b^{k-1}(x, y)) = \text{sgn}(b^{k-1}(y, z)) \neq 0$,
- c) x does not satisfy a) or b).

By Lemma 3.9, we know that $b^k(x, z) = \sum_{\ell \in \{a_i : i \in [t]\}} b^k(x, z, \ell)$ and $b^{k-1}(y, z) = \sum_{\ell \in \{a_i : i \in [t]\}} b^{k-1}(y, z, \ell)$. Thus, from the definition of μ_y and the proof of Lemma 3.9, we have that

$$b^k(x, z, \ell) = \begin{cases} -b^{k-1}(x, z, \ell) & : \text{Case a)} \\ b^{k-1}(x, y)b^{k-1}(y, z, \ell) + b^{k-1}(x, z, \ell) & : \text{Case b)} \\ b^{k-1}(x, z, \ell) & : \text{Case c)} \end{cases}$$

By induction, each expression on the right hand side of the equality is independent of the choice of $z \in \{b_i^{(j)} : i \in [r_j]\} \sqcup \{a'_j\}$. Thus $b^k(x, z, \ell)$ is independent of the choice of $z \in \{b_i^{(j)} : i \in [r_j]\} \sqcup \{a'_j\}$. \square

Lemma 3.11. Let (R, F) be a t -colored direct sum with a direct sum decomposition of the form shown in (1), let $\underline{\mu}$ be a mutation sequence of (R, F) where $\text{supp}(\underline{\mu}) \subset (Q_1)_0$, and let $k \in [0, d]$. In any $(R^{(k)}, F)$, the arrows incident to the frozen vertex a'_i (for all $i \in [t]$) have color a_i .

Proof. Let $a'_i \in \{a'_1, \dots, a'_t\}$ be given. We proceed by induction on k . If $k = 0$, no mutations have been applied so the desired result holds. Suppose the result holds $(R^{(k-1)}, F)$ and we will show that the result holds for $(R^{(k)}, F)$. We can write $(R^{(k)}, F) = (\mu_y R^{(k-1)}, F)$ for some $y \in (Q_1)_0$. As $y \neq a'_i$, there are only two cases to consider:

- b) a'_i is connected to y and there is a 2-path $a'_i \rightarrow y \rightarrow z$ or $a'_i \leftarrow y \leftarrow z$ in $(R^{(k-1)}, F)$,
- c) a'_i does not satisfy b).

First, in *Case b)*, if there is a 2-path $a'_i \rightarrow y \rightarrow z$ in $(R^{(k-1)}, F)$ (resp. $a'_i \leftarrow y \leftarrow z$ in $(R^{(k-1)}, F)$), then by induction the arrow $(a'_i \rightarrow y) \in (R^{(k-1)}, F)_1$ (resp. $(a'_i \leftarrow y) \in (R^{(k-1)}, F)_1$) has color a_i . Thus if there is a 2-path $a'_i \rightarrow y \rightarrow z$ in $(R^{(k-1)}, F)$ (resp. $a'_i \leftarrow y \leftarrow z$ in $(R^{(k-1)}, F)$), then there is an arrow $a'_i \rightarrow z \in (R^{(k)}, F)_1$ (resp. $a'_i \leftarrow z \in (R^{(k)}, F)_1$) of color a_i .

In *Case c)*, the mutation at y does not affect the arrows α connecting a'_i and any vertex $z \in (R^{(k)}, F)_0$. Therefore the color of such an arrow is inherited from its color as an arrow in $A(k-1)$. By induction, such arrows have color a_i . \square

We now arrive at the main result of this section. It shows that if \hat{Q} is a t -colored direct sum each of whose summands has a maximal green sequence, then one can build a maximal green sequence for Q using the maximal green sequences for each of its summands.

Theorem 3.12. Let $Q = Q_1 \oplus_{(a_1, \dots, a_1, \dots, a_t, \dots, a_t)}^{(b_1^{(1)}, \dots, b_{r_1}^{(1)}, \dots, b_1^{(t)}, \dots, b_{r_t}^{(t)})} Q_2$ be a t -colored direct sum of quivers. If $\underline{\mu}_1 \in \text{green}(Q_1)$ and $\underline{\mu}_2 \in \text{green}(Q_2)$, then $\underline{\mu}_2 \circ \underline{\mu}_1 \in \text{green}(Q)$.

Proof of Theorem 3.12. Let σ_i denote the permutation of the vertices of Q_i induced by $\underline{\mu}_i$. Observe that under the identification in Definition 3.1, we let

$$\hat{Q} = \hat{Q}_1 \oplus_{(a_1, \dots, a_1, \dots, a_t, \dots, a_t)}^{(b_1^{(1)}, \dots, b_{r_1}^{(1)}, \dots, b_1^{(t)}, \dots, b_{r_t}^{(t)})} \hat{Q}_2.$$

We also have that $\hat{Q}_1 \oplus_{(a_1, \dots, a_1, \dots, a_t, \dots, a_t)}^{(b_1^{(1)}, \dots, b_{r_1}^{(1)}, \dots, b_1^{(t)}, \dots, b_{r_t}^{(t)})} \hat{Q}_2$ is a t -colored direct sum of the form shown in (1).

We first show that $\underline{\mu}_1 \hat{Q}$ is a s -colored direct sum (for some s). Let $\underline{\mu}_1 = \mu_{i_d} \circ \dots \circ \mu_{i_1}$. Since $\underline{\mu}_1 \in \text{green}(Q_1)$, we have that $\underline{\mu}_1 \hat{Q}_1 = Q_1 \sigma_1$ and so for each frozen vertex a'_j with $j \in [t]$, we obtain that $x_j := a_j \cdot \sigma_1 \in (Q_1)_0$ is the unique mutable vertex of \hat{Q} that is connected to a'_j by an arrow. Furthermore, $(x_j \xleftarrow{\alpha} a'_j) \in (\underline{\mu}_1 \hat{Q})_1$ is the unique arrow of $\underline{\mu}_1 \hat{Q}$ connecting these two vertices.

By Lemma 3.9, for any a'_j we have that $b^d(x_j, a'_j) = \sum_{\ell \in \{a_i : i \in [t]\}} b^d(x_j, a'_j, \ell)$. Since $\widetilde{Q_1\sigma_1}$ has no 2-cycles, $\text{sgn}(b^d(x_j, a'_j, \ell)) \leq 0$ for any $\ell \in \{a_i : i \in [t]\}$. By Lemma 3.11, α_j has color a_j so $b^d(x_j, a'_j) = b^d(x_j, a'_j, a_j)$. By Lemma 3.10, given any $x_j := a_j \cdot \sigma_1 \in (Q_1)_0$ we have that $b^d(x_j, z) = b^d(x_j, z, a_j) = -1$ for any $z \in \{b_i^{(j)} : i \in [r_j]\} \sqcup \{a'_j\}$. Thus we have that $\underline{\mu}_1 \hat{Q} = \hat{Q}_2 \oplus_{(b_1^{(1)}, \dots, b_{r_1}^{(1)}, \dots, b_1^{(t)}, \dots, b_{r_t}^{(t)})}^{(x_1, \dots, x_1, \dots, x_t, \dots, x_t)} \widetilde{Q_1\sigma_1}$ is a s -colored direct sum where $\{b_1^{(1)}, \dots, b_{r_1}^{(1)}, \dots, b_1^{(t)}, \dots, b_{r_t}^{(t)}\}$ is a multiset on $(Q_2)_0 \setminus F_2$ (with s distinct elements) and $\{x_1, \dots, x_1, \dots, x_t, \dots, x_t\}$ is a multiset on $(Q_1)_0 \setminus F_1$. Note that in this s -colored direct sum, the $b_i^{(j)}$'s are not necessarily given in increasing order.

Next, we show that $\underline{\mu}_2(\underline{\mu}_1(\hat{Q}))$ is a t -colored direct sum. Since $\underline{\mu}_1 \hat{Q}$ is a s -colored direct sum and $\underline{\mu}_2 = \mu_{j_{d'}} \circ \dots \circ \mu_{j_1}$ is a mutation sequence with $\text{supp}(\underline{\mu}_2) \subset (Q_2)_0$, one defines coloring functions $\{g^k\}_{0 \leq k \leq d'}$ on $\underline{\mu}_1 \hat{Q}$ with respect to Q_2 in the sense of Definition 3.7. Now an analogous argument to that of the previous two paragraphs shows that

$$\underline{\mu}_2(\underline{\mu}_1(\hat{Q})) = \widetilde{Q_1\sigma_1} \oplus_{(x_1, \dots, x_1, \dots, x_t, \dots, x_t)}^{(y_1^{(1)}, \dots, y_{r_1}^{(1)}, \dots, y_1^{(t)}, \dots, y_{r_t}^{(t)})} \widetilde{Q_2\sigma_2}$$

where $y_j^{(i)} := b_j^{(i)} \cdot \sigma_2$ with $i \in [t]$, $j \in [r_i]$. One now observes that

$$(\underline{\mu}_2 \circ \underline{\mu}_1)(\hat{Q}) = \widetilde{Q_1\sigma_1} \oplus_{(x_1, \dots, x_1, \dots, x_t, \dots, x_t)}^{(y_1^{(1)}, \dots, y_{r_1}^{(1)}, \dots, y_1^{(t)}, \dots, y_{r_t}^{(t)})} \widetilde{Q_2\sigma_2} \cong \check{Q}$$

and thus all mutable vertices of $(\underline{\mu}_2 \circ \underline{\mu}_1)(\hat{Q})$ are red.

Finally, since $\underline{\mu}_i \in \text{green}(Q_i)$ for $i = 1, 2$, each mutation of \hat{Q} along $\underline{\mu}_2 \circ \underline{\mu}_1$ takes place at a green vertex. Thus $\underline{\mu}_2 \circ \underline{\mu}_1 \in \text{green}(Q)$. \square

Remark 3.13. We believe that Theorem 3.12 holds for any quiver that can be realized as the direct sum of two non-empty quivers, but we do not have a proof.

4. QUIVERS ARISING FROM TRIANGULATED SURFACES

In this section, we show that Theorem 3.12 can be applied to quivers that arise from triangulated surfaces. Our main result of this section is that quivers Q arising from triangulated surfaces can be realized as t -colored direct sums (see Corollary 4.5). Before presenting this result and its proof, we recall for the reader how a triangulated surface defines a quiver. For more details on this construction, we refer the reader to [11].

Let \mathbf{S} denote an oriented Riemann surface that may or may not have a boundary and let $\mathbf{M} \subset \mathbf{S}$ be a finite subset of \mathbf{S} where we require that for each component \mathbf{B} of $\partial\mathbf{S}$ we have $\mathbf{B} \cap \mathbf{M} \neq \emptyset$. We call the elements of \mathbf{M} **marked points**, we call the elements of $\mathbf{M} \setminus (\mathbf{M} \cap \partial\mathbf{S})$ **punctures**, and we call the pair (\mathbf{S}, \mathbf{M}) a **marked surface**. We require that (\mathbf{S}, \mathbf{M}) is not one of the following **degenerate marked surfaces**: a sphere with one, two, or three punctures; a disc with one, two, or three marked points on the boundary; or a punctured disc with one marked point on the boundary.

Given a marked surface (\mathbf{S}, \mathbf{M}) , we consider curves on \mathbf{S} up to isotopy. We define an **arc** on \mathbf{S} to be a simple curve γ in \mathbf{S} whose endpoints are marked points and which is not isotopic to a boundary component of \mathbf{S} . We say two arcs γ_1 and γ_2 on \mathbf{S} are **compatible** if they are isotopic relative to their endpoints to curves that are nonintersecting except possibly at their endpoints. A **triangulation** of \mathbf{S} is defined to be a maximal collection of pairwise compatible arcs, denoted \mathbf{T} . Each triangulation \mathbf{T} of \mathbf{S} defines a quiver $Q_{\mathbf{T}}$ by associating vertices to arcs and arrows based on oriented adjacencies (see Figure 4).

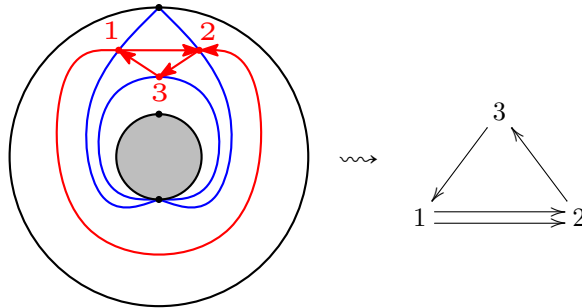


FIGURE 4. The quiver $Q_{\mathbf{T}}$ defined by a triangulation \mathbf{T} .

One can also move between different triangulations of a given marked surface (\mathbf{S}, \mathbf{M}) . Define the **flip** of an arc $\gamma \in \mathbf{T}$ to be the unique arc $\gamma' \neq \gamma$ that produces a triangulation of (\mathbf{S}, \mathbf{M}) given by $\mathbf{T}' = (\mathbf{T} \setminus \{\gamma\}) \sqcup \{\gamma'\}$ (see Figure 5). If (\mathbf{S}, \mathbf{M}) is a marked surface where \mathbf{M} contains punctures, there will be triangulations of \mathbf{S} that contain **self-folded triangles** (the region of \mathbf{S} bounded by γ_3 and γ_4 in Figure 6 is an example of a self-folded triangle). We refer to the arc γ_3 (resp. γ_4) shown in the triangulation in Figure 6 as a **loop** (a **radius**). As the flip of a radius of a self-folded triangle is not defined, Fomin, Shapiro, and Thurston introduced **tagged arcs**, a generalization of arcs, in order to develop such a notion.

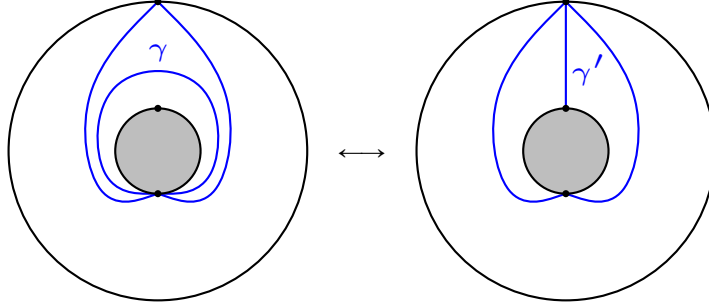


FIGURE 5. A flip connecting two triangulations of an annulus.

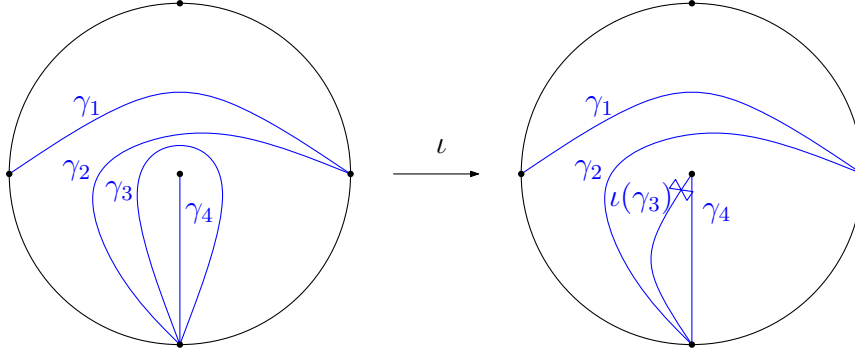


FIGURE 6. The map identifying a triangulation of a punctured disk as a tagged triangulation of a punctured disk.

We will not review the details of tagged arcs in this paper, but we remark that any triangulation can be regarded as a **tagged triangulation** of (\mathbf{S}, \mathbf{M}) (i.e. a maximal collection of pairwise compatible tagged arcs). In Figure 6, we show how one regards a triangulation of (\mathbf{S}, \mathbf{M}) as a tagged triangulation of (\mathbf{S}, \mathbf{M}) . We also note that any tagged triangulation \mathbf{T} of (\mathbf{S}, \mathbf{M}) gives rise to a quiver $Q_{\mathbf{T}}$ (see Example 8.1 for a quiver defined by a tagged triangulation or see [11] for more examples and details).

We now review the notion of blocks, which was introduced in [11] and used to classify quivers defined by a triangulation of some surface.

Definition 4.1. [11, Def. 13.1] A **block** is a directed graph isomorphic to one of the graphs shown in Figure 7. Depending on which graph it is, we call it a block of type I, II, III, IV, or V. The vertices marked by unfilled circles in Figure 7 are called outlets. A directed graph Γ is called **block-decomposable** if it can be obtained from a collection of disjoint blocks by the following procedure. Take a partial matching of the combined set of outlets; matching an outlet to itself or to another outlet from the same block is not allowed. Identify (or glue) the vertices within each pair of the matching. We require that the resulting graph Γ' be connected. If Γ' contains a pair of edges connecting the same pair of vertices but going in opposite directions, then remove each such a pair of edges. The result is a block-decomposable graph Γ .

As quivers are examples of directed graphs, one can ask if there is a description of the class of block-decomposable quivers. The following theorem answers this question completely.

Theorem 4.2. [11, Thm. 13.3] Block-decomposable quivers are exactly those quivers defined by a triangulation of some surface.

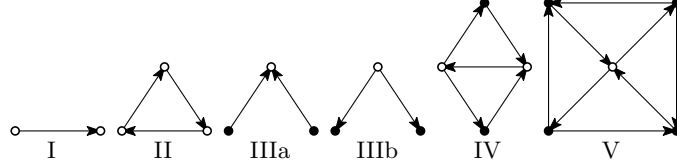


FIGURE 7. The Fomin-Shapiro-Thurston blocks.

Remark 4.3. Let $Q_{\mathbf{T}}$ be a quiver defined by a triangulated surface with no frozen vertices. In other words, we are assuming that every $v \in (Q_{\mathbf{T}})_0$ is a mutable vertex. Then

$$\begin{aligned} \#\{\alpha \in (Q_{\mathbf{T}})_1 : x \xrightarrow{\alpha} y \text{ for some } y \in (Q_{\mathbf{T}})_0\} &\leq 2 \\ \#\{\alpha \in (Q_{\mathbf{T}})_1 : y \xrightarrow{\alpha} x \text{ for some } y \in (Q_{\mathbf{T}})_0\} &\leq 2. \end{aligned}$$

We now consider the quivers that are defined by triangulations, but are not irreducible. We show that any such quiver is a t -colored direct sum. The following lemma is a crucial step in showing that a quiver defined by a triangulation that is not irreducible will not have a double arrow connecting two summands of Q .

Lemma 4.4. Assume that Q is defined by a triangulated surface (with 1 connected component) and that

$$a \begin{array}{c} \xrightarrow{\alpha_1} \\ \xrightarrow{\alpha_2} \end{array} b \quad \text{is a proper subquiver of } Q. \text{ Then there exists a path of length 2 from } b \text{ to } a.$$

Proof. Since Q is defined by a triangulated surface, there exists a block decomposition $\{R_j\}_{j \in [m]}$ of Q by Theorem 4.2. By definition of the blocks, α_1 and α_2 come from distinct blocks. Without loss of generality, α_1 is an arrow of R_1 and α_2 is an arrow of R_2 . Furthermore, in R_i with $i = 1, 2$ we must have that $s(\alpha_i)$ and $t(\alpha_i)$ are outlets. Thus R_i with $i = 1, 2$ is of type I, II, or IV, but by assumption R_1 and R_2 are not both of type I. When we glue the R_1 to R_2 to using the identifications associated with Q , a case by case analysis shows that there exists a path of length 2 from b to a . Furthermore, the vertices corresponding to a and b are no longer outlets. Thus attaching the remaining R_j 's will not delete any arrows from this path. \square

Corollary 4.5. Let Q be a quiver defined by a triangulated surface (with 1 connected component) that is not irreducible. If $Q \neq a \begin{array}{c} \xrightarrow{\alpha_1} \\ \xrightarrow{\alpha_2} \end{array} b$, then Q is a t -colored direct sum for some $t \in \mathbb{N}$.

Proof. Since we are assuming that Q is not irreducible, there exists subquivers Q_1 and Q_2 of Q such that we can write Q as the direct sum $Q = Q_1 \oplus_{(a_1, \dots, a_k)}^{(b_1, \dots, b_k)} Q_2$ where $\{a_1, \dots, a_k\}$ is a multiset on $(Q_1)_0$ and $\{b_1, \dots, b_k\}$ is a multiset on $(Q_2)_0$. Let $a_i \in \{a_1, \dots, a_k\}$ and $b_j \in \{b_1, \dots, b_k\}$ be given. We claim that $\#\{\alpha \in (Q)_1 : a_i \xrightarrow{\alpha} b_j\} \leq 1$.

Suppose this were not the case, then Q would have a proper subquiver of the form $a_i \begin{array}{c} \xrightarrow{\alpha_1} \\ \xrightarrow{\alpha_2} \end{array} b_j$. By

Lemma 4.4, there must be a path of length 2 from b_j to a_i . This contradicts the fact that all arrows between $\{a_1, \dots, a_k\}$ and $\{b_1, \dots, b_k\}$ point towards the latter. Hence, Q is not only a direct sum but is a t -colored direct sum. \square

5. SIGNED IRREDUCIBLE TYPE \mathbb{A} QUIVERS

In this section, we focus our attention on **type \mathbb{A}_n quivers**, which are defined to be quivers $R \in \text{Mut}(1 \leftarrow 2 \leftarrow \dots \leftarrow n)$ where $n \geq 1$ is a positive integer. We begin by classifying irreducible type \mathbb{A}_n quivers. After that, we explain how almost any irreducible type \mathbb{A}_n quiver carries the structure of a binary tree of 3-cycles. In section 6, we will show how regarding irreducible type \mathbb{A}_n quivers as trees of 3-cycles allows us to construct maximal green sequences for such quivers.

Our first step in classifying irreducible type \mathbb{A}_n quivers is to present the following theorem of Buan and Vatne, which classifies quivers in $\text{Mut}(1 \leftarrow 2 \leftarrow \dots \leftarrow n)$ where $n \geq 1$ is a positive integer. We will say that a quiver is of **type \mathbb{A}** if it is of type \mathbb{A}_n for some positive integer $n \geq 1$.

Lemma 5.1. [6, Prop. 2.4] A quiver Q is of type \mathbb{A} if and only if Q satisfies the following:

- i) all non-trivial cycles in the underlying graph of Q are of length 3 and are oriented in Q ,
- ii) any vertex has at most four neighbors,

- iii) if a vertex has four neighbors, then two of its adjacent arrows belong to one 3-cycle, and the other two belong to another 3-cycle,
- iv) if a vertex has exactly three neighbors, then two of its adjacent arrows belong to one 3-cycle, and the third arrow does not belong to any 3-cycle.

Corollary 5.2. Besides the quiver of type \mathbb{A}_1 , the *irreducible* quivers of type \mathbb{A} are exactly those quivers Q obtained by gluing together a finite number of Type II blocks $\{S_\alpha\}_{\alpha \in [n]}$ in such a way that the cycles in the underlying graph of Q are in bijection with the elements of $\{S_\alpha\}_{\alpha \in [n]}$. Additionally, each S_α shares a vertex with at most three other S_β 's. (We say that S_α is **connected** to S_β in such a situation.)

Proof. Assume that Q is a quiver obtained by gluing together a finite number of Type II blocks $\{S_\alpha\}_{\alpha \in [n]}$ in such a way that the cycles in the underlying graph of Q are in bijection with the elements of $\{S_\alpha\}_{\alpha \in [n]}$. Then Q satisfies *i*) in Lemma 5.1. By the rules for gluing blocks together, each vertex $i \in (Q)_0$ has either two or four neighbors so *ii*) and *iv*) in Lemma 5.1 hold. It also follows from the gluing rules that if i has four neighbors, then two of its adjacent arrows belong to one 3-cycle and the other two belong to another 3-cycle so *iii*) in Lemma 5.1 holds. Additionally, since each arrow of Q is contained in an oriented 3-cycle, there is no way to partition the vertices into two components so that the arrows connecting them coherently point from one to the other. Thus the quiver Q is irreducible.

Conversely, let Q be an irreducible type \mathbb{A} quiver that is not the quiver of type \mathbb{A}_1 . We first show that any arrow of Q belongs to a (necessarily) oriented 3-cycle of Q . Suppose $(i \xrightarrow{\alpha} j) \in (Q)_1$ does not belong to an oriented 3-cycle of Q . Then there exist nonempty full subquivers Q_1 and Q_2 of Q such that $Q = Q_1 \oplus_{(i)}^{(j)} Q_2$. (By property *i*), there cannot be an (undirected) cycle of length larger than 3.) This contradicts the fact that Q is irreducible.

Not only is it true that every arrow of Q belongs to an oriented 3-cycle of Q , property *i*) also ensures that Q is obtained by identifying certain vertices of Type II blocks in a finite set of Type II blocks $\{S_\alpha\}_{\alpha \in [n]}$. Furthermore, property *ii*) in Lemma 5.1 implies these identifications are such that all vertices have two or four neighbors. By properties *i*) and *iii*), these identifications do not create any new cycles in the underlying graph of Q . Thus Q is obtained by gluing together a finite number of Type II blocks $\{S_\alpha\}_{\alpha \in [n]}$ in such a way that the cycles in the underlying graph of Q are in bijection with the elements of $\{S_\alpha\}_{\alpha \in [n]}$. \square

Definition 5.3. Let Q be an irreducible type \mathbb{A} quiver with at least one 3-cycle. Define a **leaf** 3-cycle S_α in Q to be a 3-cycle in Q that is connected to at most one other 3-cycle in Q . We define a **root** 3-cycle to be a chosen leaf 3-cycle.

Lemma 5.4. Suppose Q is an irreducible type \mathbb{A} quiver with at least one 3-cycle. Then Q has a leaf 3-cycle.

Proof. If Q has exactly one 3-cycle R , then $Q = R$ is a leaf 3-cycle. If Q is obtained from the Type II blocks $\{S_i\}_{i \in [n]}$, consider the block S_{i_1} . If S_{i_1} is connected to only one other 3-cycle, then S_{i_1} is a leaf 3-cycle. If S_{i_1} is connected to more than one 3-cycle, let S_{i_2} denote one of the 3-cycles to which S_{i_1} is connected. If S_{i_2} is only connected to S_{i_1} , then S_{i_2} is a leaf 3-cycle. Otherwise, there exists a 3-cycle $S_{i_3} \neq S_{i_1}$ connected to S_{i_2} . By Lemma 5.1 there are no non-trivial cycles in the underlying graph of Q besides those determined by the blocks $\{S_i\}_{i \in [n]}$ so this process will end. Thus Q has a leaf 3-cycle. \square

Consider a pair, (Q, S) where Q is an irreducible type \mathbb{A} quiver Q with at least one 3-cycle, and S denotes a root 3-cycle in Q . We now define a labeling of the arrows of Q , an ordering of the 3-cycles, and a sign function on the set of 3-cycles of Q . Adding this additional data to (Q, S) yields a binary tree structure on the set of 3-cycles $\{S_\alpha\}_{\alpha \in [n]}$.

We begin by letting $S_1 := S$ denote the chosen root 3-cycle, S_2 denote the unique 3-cycle connected to S_1 , and z_1 denote the vertex shared by S_1 and S_2 . (In the event that Q is a single 3-cycle, we choose z_1 to be a vertex of S_1 arbitrarily.) Next, we let α_1, β_1 and γ_1 denote the three arrows of S_1 in cyclic order such that $s(\gamma_1) = z_1 = t(\beta_1)$, $s(\beta_1) = t(\alpha_1)$, and $s(\alpha_1) = t(\gamma_1)$. We next label the arrows of S_2 such that $s(\alpha_2) = z_1 = t(\gamma_2)$, $t(\alpha_2) = s(\beta_2)$, and $t(\beta_2) = s(\gamma_2)$. See Figure 8 for examples of this labeling.

For $i \geq 2$, we order the remaining 3-cycles by a depth-first ordering where we

- (1) inductively define S_{i+1} to be the 3-cycle attached to the vertex $t(\alpha_i)$,
- (2) define α_{i+1} such that $s(\alpha_{i+1}) = t(\alpha_i)$ and then $\beta_{i+1}, \gamma_{i+1}$ follow α_{i+1} in cyclic order,
- (3) if no 3-cycle is attached to $t(\alpha_i)$, define S_{i+1} to be the 3-cycle attached to $t(\beta_i)$ and $s(\alpha_{i+1}) = t(\beta_i)$ instead, and finally
- (4) minimally backtrack and continue the depth-first ordering until all arrows and 3-cycles have been labeled.

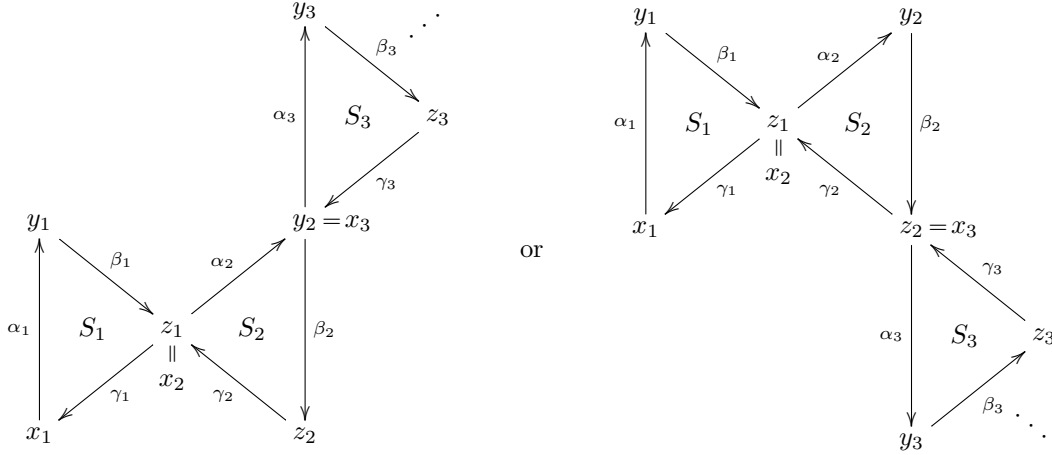


FIGURE 8. Labeling arrows of an irreducible quiver of type \mathbb{A} .

Given a 3-cycle S_i in the block decomposition of Q , define $x_i := s(\alpha_i)$, $y_i := s(\beta_i)$, and $z_i := s(\gamma_i)$. The vertex z_1 of S_1 was already defined in the previous paragraph and that definition of z_1 clearly agrees with this one. We say that a 3-cycle S_i is **positive** (resp. **negative**) if $s(\alpha_i) = t(\alpha_j)$ (resp. $s(\alpha_i) = t(\beta_j)$) for some $j < i$. We define $\text{sgn}(S_i) := +$ (resp. $-$) if S_i is positive (resp. negative). By convention, we set $\text{sgn}(S_1) = +$. We define $T_i := (S_i, \text{sgn}(S_i))$ to be a 3-cycle in the block decomposition of Q and its sign. We will refer to T_i where $i \in [n]$ as a **signed 3-cycle** of Q . For graphical convenience, we will consistently draw 3-cycles as shown in Figure 9 with the convention that $\text{sgn}(S_i) = +$ (resp. $-$) in the former figure (resp. latter figure). We refer to the data $\mathcal{Q} := (Q, S, \{T_i\}_{i \in [n]})$ as a **signed irreducible type \mathbb{A} quiver**.

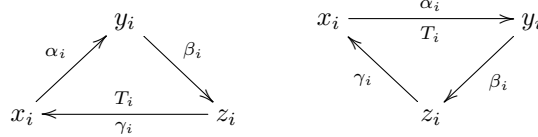


FIGURE 9. A positive (resp. negative) 3-cycle is shown on the left (resp. right).

Remark 5.5. If Q is an irreducible type \mathbb{A} quiver with more than one 3-cycle, then the choice of a root 3-cycle completely determines the sign of each 3-cycle of Q . Thus $\mathcal{Q} = (Q, S, \{T_i\}_{i \in [n]})$ depends only on (Q, S) and thus it makes sense to refer to the signed irreducible type \mathbb{A} quiver *defined by* (Q, S) .

The next lemma follows immediately from Corollary 5.2 and from our definition of the sign of a 3-cycle S_i in Q .

Lemma 5.6. If Q is an irreducible type \mathbb{A} quiver with at least one 3-cycle, S is a root 3-cycle of Q and $\mathcal{Q} = (Q, S, \{T_i\}_{i \in [n]})$ is a signed irreducible type \mathbb{A} quiver defined by (Q, S) , then \mathcal{Q} is equivalent to a labeled binary tree with vertex set $\{S_i\}_{i \in [n]}$ where S_i is connected to S_j by an edge if and only if S_i is connected to S_j (i.e. S_i and S_j share a vertex). Furthermore, a 3-cycle $S_j \in \{S_i\}_{i \in [n]}$ has a right child (resp. left child) if and only if S_j shares the vertex y_j (resp. z_j) with another 3-cycle, .

For the remainder of this section, we assume that Q is a given irreducible type \mathbb{A} quiver and S a root 3-cycle of Q . We also assume \mathcal{Q} is a signed irreducible type \mathbb{A} defined by the data (Q, S) . For convenience, we will abuse notation and refer to the **vertices**, **arrows**, **3-cycles**, etc. of \mathcal{Q} with the understanding that we are referring to the vertices, arrows, 3-cycles, etc. of Q , respectively. Since we will often work with $\hat{\mathcal{Q}}$, the framed quiver of Q , it will also be useful to define $\hat{\mathcal{Q}}$ to be framed quiver of Q with the additional data of S , the root 3-cycle of Q , and the data of a sign associated with each 3-cycle of Q . Now for convenience, we will abuse notation and refer to the **mutable vertices**, **frozen vertices**, **arrows**, and **3-cycles** of $\hat{\mathcal{Q}}$ with the understanding that we are referring to the mutable vertices, frozen vertices, arrows, and 3-cycles of $\hat{\mathcal{Q}}$, respectively. We will refer to $\hat{\mathcal{Q}}$

as a **signed irreducible type \mathbb{A} framed quiver**. Additionally, we define a **full subquiver** \mathcal{R} of \mathcal{Q} or $\hat{\mathcal{Q}}$ to be a full subquiver of \mathcal{Q} or $\hat{\mathcal{Q}}$, respectively, with the property that the sign of any 3-cycle C of \mathcal{R} is the same as the sign of C when regarded as a 3-cycle of \mathcal{Q} or $\hat{\mathcal{Q}}$.

Example 5.7. In Figure 10, we show an example of a signed irreducible type \mathbb{A}_{23} quiver, which we denote by \mathcal{Q} . The positive 3-cycles of \mathcal{Q} are T_1, T_3, T_4, T_5, T_7 . For clarity, we have labeled the arrows of \mathcal{Q} in Figure 10, but we will often suppress these labels in later examples. We also note that many of the vertices, e.g. z_1, y_2, y_3, z_3 could also be labeled as x_2, x_3, x_4, x_{11} , respectively, but we suppress the vertex labels x_i (which are shorthand for $s(\alpha_i)$) except for x_1 .

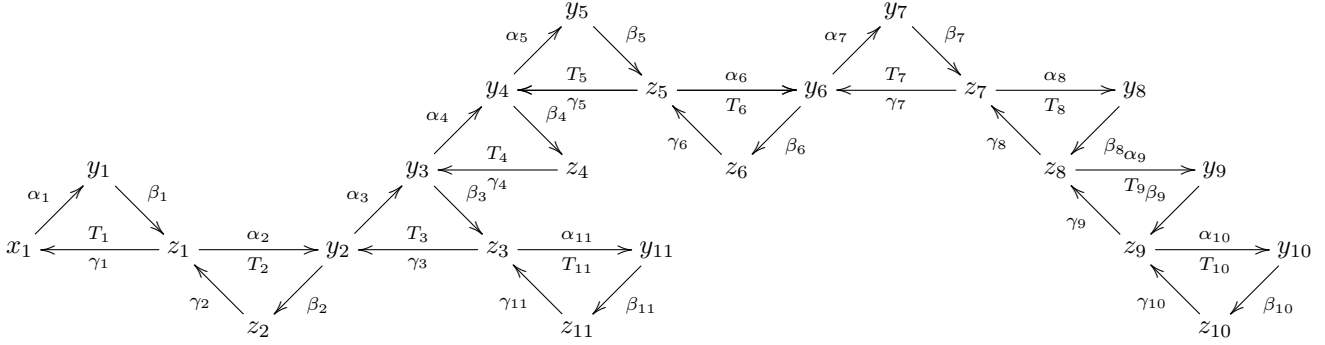


FIGURE 10. A signed irreducible type \mathbb{A}_{23} quiver.

It will be helpful to define an ordering on the vertices of $\hat{\mathcal{Q}}$. We label the mutable vertices of $\hat{\mathcal{Q}}$ according to the linear order

$$1 = s(\alpha_1) < t(\alpha_1) < t(\beta_1) < t(\alpha_2) < t(\beta_2) < \dots < t(\alpha_n) < t(\beta_n) = N$$

and the frozen vertices of $\hat{\mathcal{Q}}$ according to the linear order

$$N + 1 = s(\alpha_1)' < t(\alpha_1)' < t(\beta_1)' < t(\alpha_2)' < t(\beta_2)' < \dots < t(\alpha_n)' < t(\beta_n)' = 2N.$$

We call this the **standard ordering** of the vertices of $\hat{\mathcal{Q}}$.

Example 5.8. Let $\hat{\mathcal{Q}}$ denote the signed irreducible type \mathbb{A}_{23} framed quiver shown in Figure 11. We have labeled the vertices of $\hat{\mathcal{Q}}$ in Figure 11 according to the standard ordering. Note that we have suppressed the arrow labels in Figure 11.

6. ASSOCIATED MUTATION SEQUENCES

Throughout this section we work with a given signed irreducible type \mathbb{A} quiver \mathcal{Q} with respect to a fixed root 3-cycle S . Based on the data defining the signed irreducible type \mathbb{A} quiver \mathcal{Q} , we construct a mutation sequence of \mathcal{Q} that we will call the **associated mutation sequence** of \mathcal{Q} . After that we state our main theorem which says that the associated mutation sequence of \mathcal{Q} is a maximal green sequence (see Theorem 6.5). We then apply our main theorem to construct a maximal green sequence for any type \mathbb{A} quiver \mathcal{Q} (see Corollary 6.8).

6.1. Definition of Associated Mutation Sequences. Before defining the associated mutation sequence of \mathcal{Q} , we need to develop some terminology.

Definition 6.1. Let T_k be a signed 3-cycle of \mathcal{Q} . Define the sequence of vertices $(x(0, k), x(1, k), \dots, x(d, k))$ of \mathcal{Q} by

$$x(j, k) := \begin{cases} z_k & : \text{ if } j = 0, \\ t(\gamma_{m_j}) & : \gamma_{m_j} \text{ is the unique arrow of } \mathcal{Q} \text{ satisfying } s(\gamma_{m_j}) = x(j-1, k). \end{cases}$$

Note that such a sequence is necessarily finite, and we choose d to be maximal, or equivalently so that $\text{sgn}(S_{m_d}) = +$. When k is clear from context, we abbreviate $x(s, k)$ as $x(s)$. It follows from the definition of $x(j)$ that $x(j) = x_{m_j}$ for any $j \in [d]$, and that $x(d) = x_1$ or y_{m_d-1} . However, $x(0)$ can be expressed as x_s for some $s \in [n]$ only if $\deg(x(0)) = \deg(z_k) = 4$. See Figure 12. Note that if $\text{sgn}(S_k) = +$, then this sequence of vertices is simply $(x(0), x(1))$.

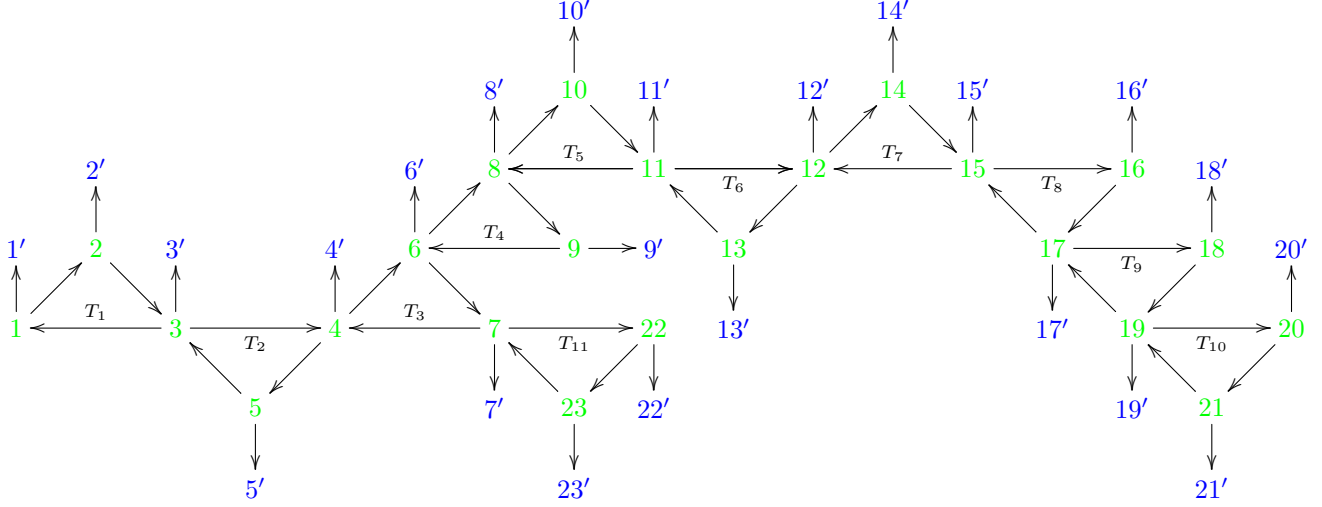


FIGURE 11. The framed quiver of a signed irreducible type A_{23} quiver with vertices labeled using the standard ordering.

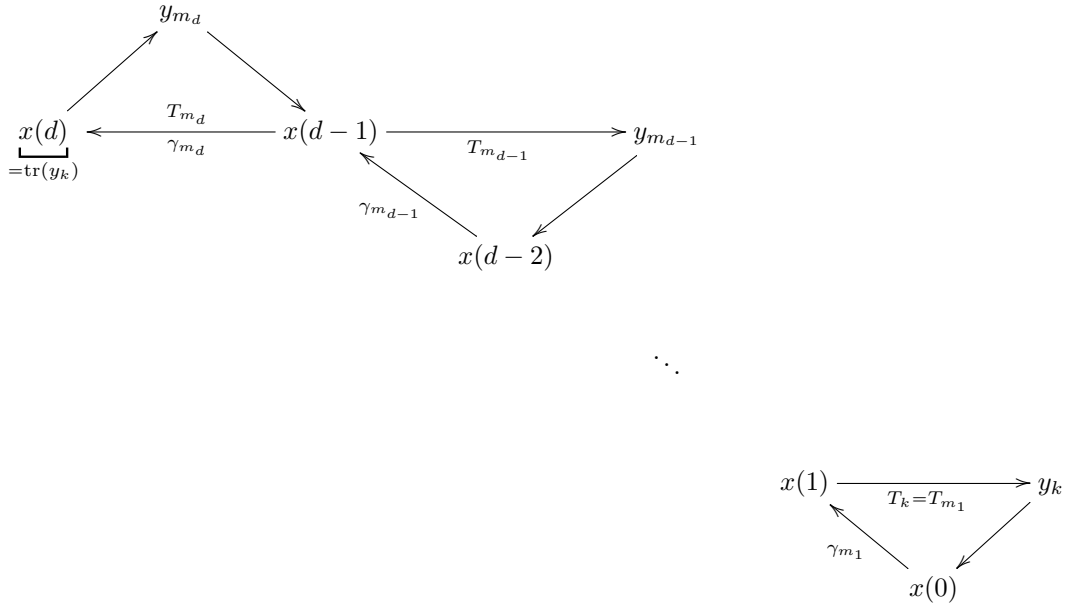


FIGURE 12. The sequence $(x(0), x(1), \dots, x(d))$ defined by T_k where $\text{sgn}(S_k) = -$. The transport of y_k is also illustrated for quivers where there is no sequence of the form in (2) of Definition 6.2.

Definition 6.2. For any vertex v of Q which can be expressed as $v = y_k$, i.e. as a point of some signed 3-cycle T_k of \mathcal{Q} , we define the **transport** of y_k by the following procedure. We will denote the image of the transport as $\text{tr}(v)$. Consider the full subquiver of \mathcal{Q} on the vertices of the signed 3-cycles T_1, T_2, \dots, T_k , which we denote by \mathcal{Q}_k . Inside this subquiver,

- i) move from y_k along β_k to $t(\beta_k)$,
- ii) move from $t(\beta_k)$ along the sequence of arrows $\gamma_{m_1}, \gamma_{m_2}, \dots, \gamma_{m_d}$ of maximal length to $t(\gamma_{m_d})$ where the integers $\{m_i\}_{i \in [d]}$ are those defined by the signed 3-cycle T_k (see Definition 6.1),
- iii) if possible, move from $t(\gamma_{m_d})$ to $\text{tr}(y_k) := t(\beta_{k_s})$ along the sequence of arrows of the form shown in (2) each of which belongs to a signed 3-cycle T_i for some $i < k$, under the assumption that the subsequences

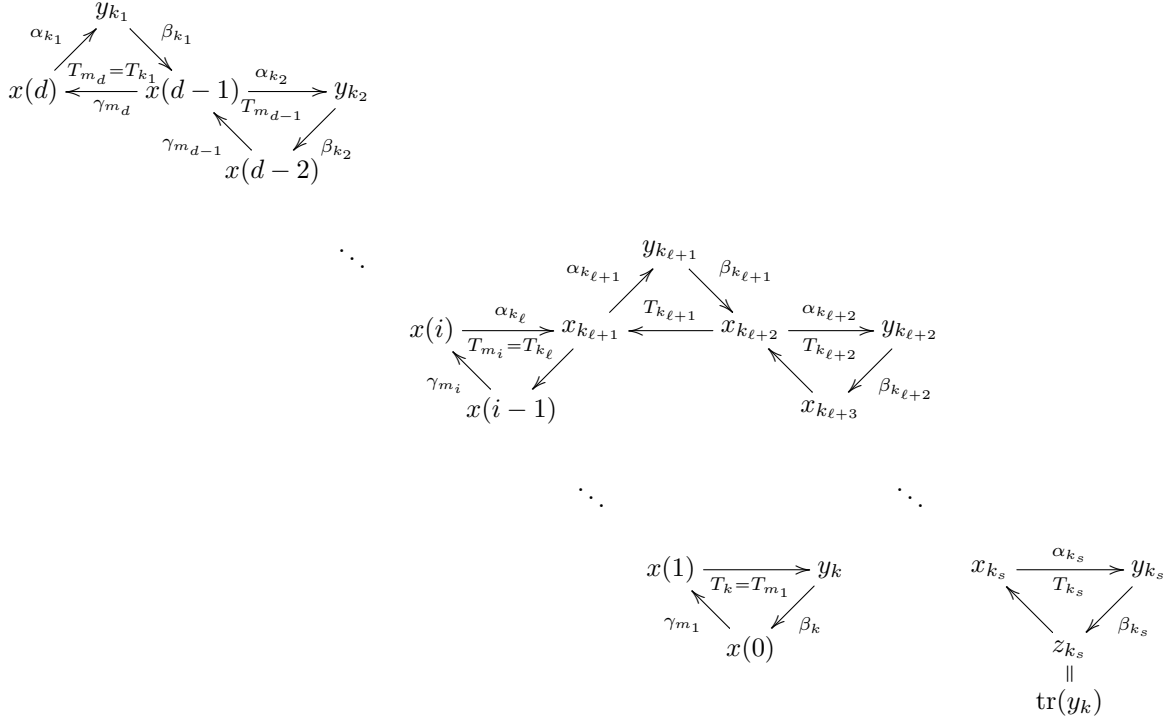


FIGURE 13. The sequence of arrows one follows to compute the transport of y_k . Note that in this case, the sequence A_1 is non-empty.

A_1 and A_2 are of maximal length, and A_2 must be nonempty. If no such sequence exists of this form, we instead define $\text{tr}(y_k) := t(\gamma_{m_d})$.

$$(2) \quad \underbrace{\alpha_{k_1}, \beta_{k_1}, \alpha_{k_2}, \beta_{k_2}, \dots, \alpha_{k_{\ell-1}}, \beta_{k_{\ell-1}}, \alpha_{k_{\ell}}, \alpha_{k_{\ell+1}}, \beta_{k_{\ell+1}}, \alpha_{k_{\ell+2}}, \beta_{k_{\ell+2}}, \dots, \alpha_{k_s}, \beta_{k_s}}_{A_1} \quad \underbrace{\alpha_{k_{\ell+1}}, \beta_{k_{\ell+1}}, \alpha_{k_{\ell+2}}, \beta_{k_{\ell+2}}, \dots, \alpha_{k_s}, \beta_{k_s}}_{A_2}$$

See Figures 12, 13, and 14.

We now use the above notation to define the **associated mutation sequence** of \mathcal{Q} .

Definition 6.3. Let $\mathcal{Q} = (Q, S, \{T_i\}_{i \in [n]})$ be a signed irreducible type \mathbb{A} quiver. Define $\underline{\mu}_0 := \mu_{x_1}$. For each $k \in [n]$ we define a sequence of mutations, denoted $\underline{\mu}_k$, as follows. Note that when we write \emptyset below we mean the empty mutation sequence. We define

$$\underline{\mu}_k := \underline{\mu}_A \circ \underline{\mu}_B \circ \underline{\mu}_C \circ \underline{\mu}_D$$

where $\underline{\mu}_A, \underline{\mu}_B, \underline{\mu}_C$, and $\underline{\mu}_D$ are mutation sequences defined in the following way

$$\begin{aligned} \underline{\mu}_D &:= \mu_{y_k} \\ \underline{\mu}_C &:= \mu_{x(d-1)} \circ \dots \circ \mu_{x(1)} \circ \mu_{x(0)} \\ \underline{\mu}_B &:= \begin{cases} \mu_{\text{tr}(x(d))} & : \text{ if } x(d) \neq x_1 \\ \emptyset & : \text{ if } x(d) = x_1 \end{cases} \\ \underline{\mu}_A &:= \mu_{\text{tr}(y_k)}. \end{aligned}$$

Note that $x(d) = x_1$ or y_{m_d-1} so the transport $\text{tr}(x(d))$ in $\underline{\mu}_B$ is well-defined. Now define the **associated mutation sequence** of \mathcal{Q} to be $\underline{\mu} := \underline{\mu}_n \circ \dots \circ \underline{\mu}_1 \circ \underline{\mu}_0$. We will denote the associated mutation sequence of \mathcal{Q} by $\underline{\mu}$ or by $\underline{\mu}^{\mathcal{Q}}$ if it is not clear from context which signed irreducible type \mathbb{A} quiver defines $\underline{\mu}$. At times it will be useful to write $\underline{\mu}_k = \underline{\mu}_{A(k)} \circ \underline{\mu}_{B(k)} \circ \underline{\mu}_{C(k)} \circ \underline{\mu}_{D(k)}$.

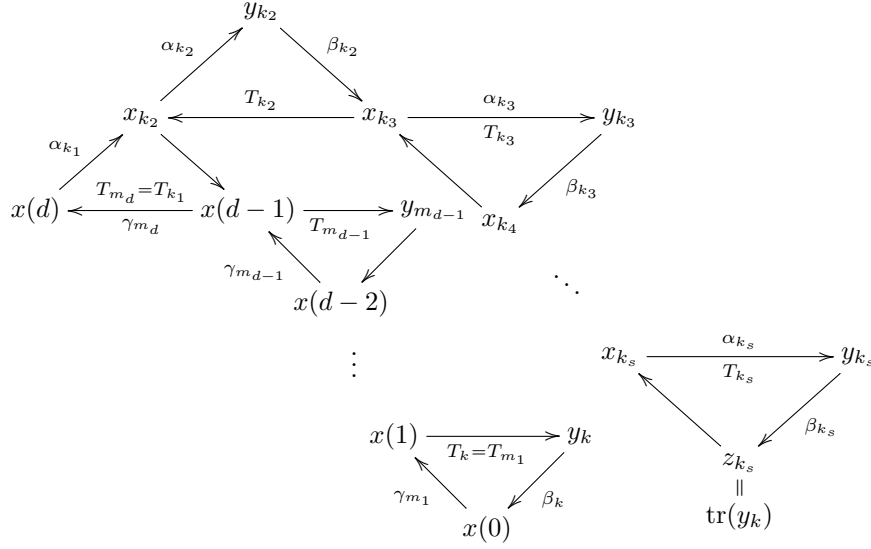


FIGURE 14. The sequence of arrows one follows to compute the transport of y_k . Note that in this case, the sequence A_1 is empty.

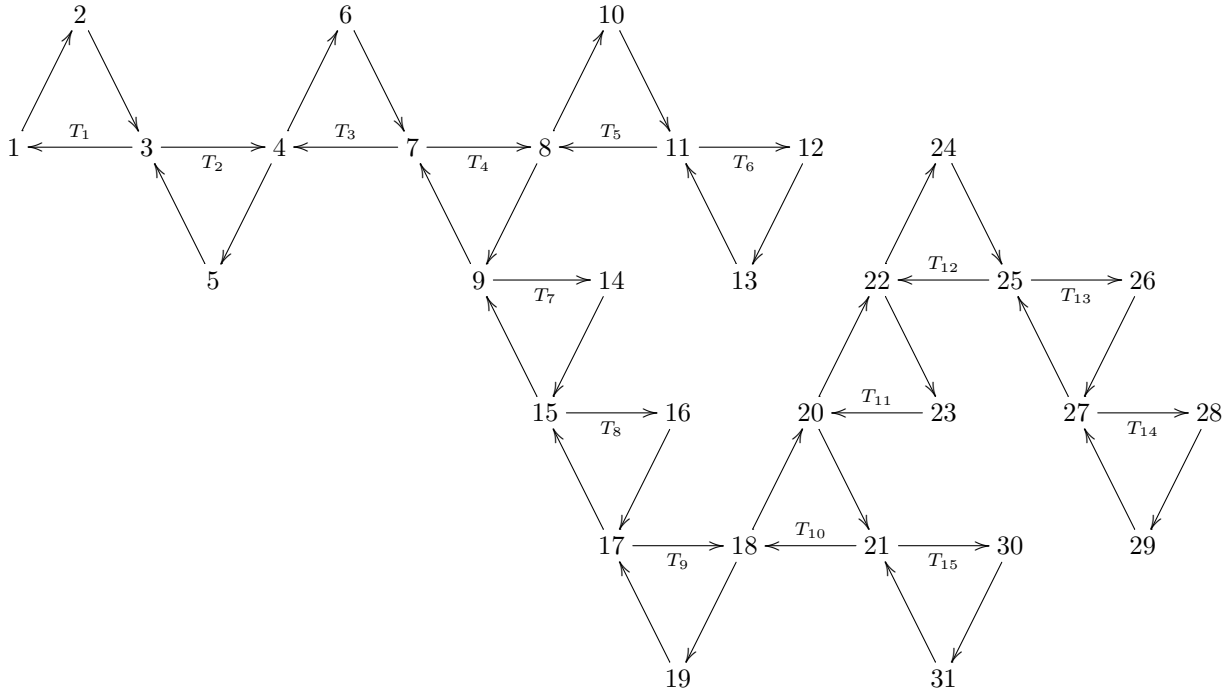


FIGURE 15. The signed irreducible type A_{31} quiver described in Example 6.4.

Example 6.4. Let \mathcal{Q} denote the signed irreducible type A_{31} quiver appearing in Figure 15. In the table in Figure 16, we describe $\underline{\mu}_i$ for each $0 \leq i \leq 15$. Thus, the associated mutation sequence defined by \mathcal{Q} is $\underline{\mu}_{15} \circ \underline{\mu}_{14} \circ \cdots \circ \underline{\mu}_1 \circ \underline{\mu}_0$.

We now arrive at the main result of this paper.

Theorem 6.5. If $\mathcal{Q} = (Q, S, \{T_i\}_{i \in [n]})$ is a signed irreducible type A quiver with associated mutation sequence $\underline{\mu}$, then we have $\underline{\mu} \in \text{green}(Q)$.

We present the proof Theorem 6.5 in the next section, as the argument requires some additional tools.

i	$\underline{\mu}_i$	i	$\underline{\mu}_i$
0	μ_1	8	$\mu_{13} \circ \mu_1 \circ \mu_7 \circ \mu_9 \circ \mu_{15} \circ \mu_{17} \circ \mu_{16}$
1	$\mu_1 \circ \mu_3 \circ \mu_2$	9	$\mu_{13} \circ \mu_1 \circ \mu_7 \circ \mu_9 \circ \mu_{15} \circ \mu_{17} \circ \mu_{19} \circ \mu_{18}$
2	$\mu_1 \circ \mu_3 \circ \mu_5 \circ \mu_4$	10	$\mu_{18} \circ \mu_{13} \circ \mu_{21} \circ \mu_{20}$
3	$\mu_4 \circ \mu_1 \circ \mu_7 \circ \mu_6$	11	$\mu_{20} \circ \mu_{18} \circ \mu_{23} \circ \mu_{22}$
4	$\mu_4 \circ \mu_1 \circ \mu_7 \circ \mu_9 \circ \mu_8$	12	$\mu_{22} \circ \mu_{20} \circ \mu_{25} \circ \mu_{24}$
5	$\mu_8 \circ \mu_4 \circ \mu_{11} \circ \mu_{10}$	13	$\mu_{22} \circ \mu_{20} \circ \mu_{25} \circ \mu_{27} \circ \mu_{26}$
6	$\mu_8 \circ \mu_4 \circ \mu_{11} \circ \mu_{13} \circ \mu_{12}$	14	$\mu_{22} \circ \mu_{20} \circ \mu_{25} \circ \mu_{27} \circ \mu_{29} \circ \mu_{28}$
7	$\mu_{13} \circ \mu_1 \circ \mu_7 \circ \mu_9 \circ \mu_{15} \circ \mu_{14}$	15	$\mu_{23} \circ \mu_{13} \circ \mu_{21} \circ \mu_{31} \circ \mu_{30}$

FIGURE 16. The associated mutation of the signed irreducible type \mathbb{A}_{31} quiver in Figure 15.

Remark 6.6. For a given irreducible type \mathbb{A} quiver with at least one 3-cycle, the length of $\underline{\mu}$ can vary depending on the choice of leaf 3-cycle. Let Q denote the irreducible type \mathbb{A}_7 quiver shown in Figure 17. By choosing the 3-cycle 1,2,3 (resp. 5,6,7) to be the root 3-cycle, one obtains the signed irreducible type \mathbb{A} quiver \mathcal{Q}_1 (resp. \mathcal{Q}_2) shown in Figure 18. Then the associated mutations of \mathcal{Q}_1 and \mathcal{Q}_2 are

$$\begin{aligned}\underline{\mu}^{\mathcal{Q}_1} &= \mu_1 \circ \mu_3 \circ \mu_5 \circ \mu_7 \circ \mu_6 \circ \mu_1 \circ \mu_3 \circ \mu_5 \circ \mu_4 \circ \mu_1 \circ \mu_3 \circ \mu_2 \circ \mu_1 \\ \underline{\mu}^{\mathcal{Q}_2} &= \mu_3 \circ \mu_6 \circ \mu_2 \circ \mu_1 \circ \mu_6 \circ \mu_5 \circ \mu_4 \circ \mu_3 \circ \mu_6 \circ \mu_5 \circ \mu_7 \circ \mu_6.\end{aligned}$$

Furthermore, the maximal green sequence produced by Theorem 6.5, i.e. the associated mutation sequence of a each signed irreducible type \mathbb{A} quiver associated to Q , is not necessarily a minimal length maximal green sequence. For example, it is easy to check that $\underline{\nu} = \mu_3 \circ \mu_1 \circ \mu_4 \circ \mu_3 \circ \mu_7 \circ \mu_6 \circ \mu_2 \circ \mu_5 \circ \mu_1 \circ \mu_4 \circ \mu_7$ is a maximal green sequence of Q , which is of length less than that of $\underline{\mu}^{\mathcal{Q}_1}$ or $\underline{\mu}^{\mathcal{Q}_2}$.

Remark 6.7. While we were revising this paper, Cormier, Dillery, Resh, Serhiyenko, and Whelan [9] found a construction of minimal length maximal green sequences for type \mathbb{A} quivers. Therein, they construct a maximal green sequence for any irreducible type \mathbb{A} quiver Q with at least one 3-cycle by mutating first at all leaf 3-cycles of Q , then mutating at the 3-cycles connected to the leaf 3-cycles of Q , continuing this process, and then mutating a subsequence of the vertices in reverse. This contrasts with the maximal green sequences we construct in this paper, which involve some extraneous steps but whose process can be defined locally and inductively, akin to writing down the reduced word for a permutation using bubble sort.

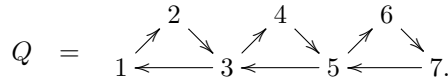


FIGURE 17.

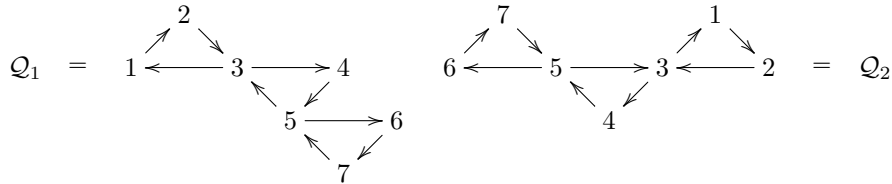


FIGURE 18. The two signed irreducible type \mathbb{A} quivers that can be obtained from Q .

We conclude this section by using Theorem 6.5 to show that any type \mathbb{A} quiver has at least one maximal green sequence.

Corollary 6.8. Let $Q \in \text{Mut}(1 \rightarrow 2 \rightarrow \dots \rightarrow n)$. Then Q has a maximal green sequence.

Proof. By Corollary 4.5, Q can be expressed as a direct sum of irreducible type \mathbb{A} quivers $\{Q_1, Q_2, \dots, Q_k\}$. In other words,

$$Q = Q_1 \oplus_{(a_{(1,1)}, b_{(2,1)}, \dots, b_{(d_1,1)})}^{(b_{(1,1)}, b_{(2,1)}, \dots, b_{(d_1,1)})} Q'_2 \text{ where } Q'_j = Q_j \oplus_{(a_{(1,j)}, a_{(2,j)}, \dots, a_{(d_j,j)})}^{(b_{(1,j)}, b_{(2,j)}, \dots, b_{(d_j,j)})} Q'_{j+1} \text{ for } 2 \leq j \leq k-1, \text{ and } Q'_k = Q_k.$$

If Q_i is of type \mathbb{A}_1 and a_i denotes the unique vertex of Q_i , then $\underline{\mu}^{(i)} := \mu_{a_i}$ is a maximal green sequence of Q_i . If Q_i is not of type \mathbb{A}_1 , then we form a signed irreducible type \mathbb{A} quiver, $\mathcal{Q}^{(i)}$, associated to Q_i by picking a leaf 3-cycle. Now by Theorem 6.5, the associated mutation sequence of $\mathcal{Q}^{(i)}$, denoted $\underline{\mu}^{(i)}$, is a maximal green sequence of Q_i . By applying Proposition 3.12 iteratively, we obtain $\underline{\mu} = \underline{\mu}^{(k)} \circ \dots \circ \underline{\mu}^{(2)} \circ \underline{\mu}^{(1)}$ is a maximal green sequence of \hat{Q} . \square

7. PROOF OF THEOREM 6.5

In this section, we work with a fixed signed irreducible type \mathbb{A} quiver $\mathcal{Q} = (Q, S, \{T_i\}_{i \in [n]})$ with N vertices. We write $\underline{\mu} = \underline{\mu}_n \circ \dots \circ \underline{\mu}_1 \circ \underline{\mu}_0$ for the associated mutation sequence of \mathcal{Q} .

Definition 7.1. For each $\underline{\mu}_i$ appearing in $\underline{\mu}$ we define a permutation $\tau_i \in \mathfrak{S}_{(\mathcal{Q})_0} \cong \mathfrak{S}_N$ where $\mathfrak{S}_{(\mathcal{Q})_0}$ denotes the symmetric group on the vertices of \mathcal{Q} . In the special case where $i = 0$, we define τ_0 to be the identity permutation. Then for $i \in [n]$ where $\underline{\mu}_i = \mu_{i_d} \circ \dots \circ \mu_{i_1}$ we define $\tau_i := (i_2, \dots, i_d)$ in cycle notation (i.e. $i_j \cdot \tau_i = i_{j+1}$ for $j \in [d-1]$ and $i_d \cdot \tau_i = i_2$). Note that $i_1 = y_i$. We also define

$$\begin{aligned} \sigma_i &:= \tau_i \cdots \tau_1 \tau_0 \\ &= \tau_i \cdots \tau_1 \end{aligned}$$

where the last equality holds since τ_0 is the identity permutation. We say that σ_n is the **associated permutation** corresponding to \mathcal{Q} .

Theorem 6.5 will imply that the associated permutation σ_n is exactly the permutation induced by $\underline{\mu}$ (see the last paragraph of Section 2).

Let T_k and T_t where $k \leq t$ be signed 3-cycles of \mathcal{Q} . Let $\mathcal{Q}_{k,t}$ denote the full subquiver of \mathcal{Q} on the vertices of T_1, \dots, T_k and the vertices of T_{m_1}, \dots, T_{m_d} where the integers $m_1, \dots, m_d \in [n]$ are those defined by T_t as in Definition 6.1. For example, $\mathcal{Q}_{k,k}$ is the full subquiver of \mathcal{Q} on the vertices of the signed 3-cycles T_1, \dots, T_k . By convention, we also define $\mathcal{Q}_{0,0}$ to be the full subquiver of \mathcal{Q} consisting of only the vertex x_1 . Now define $\text{tr}|_{k,t}$ to be the restriction of the transport to $\mathcal{Q}_{k,t}$.

Lemma 7.2. For each $k \in [n]$ there is an ice quiver \bar{R}_k that is a full subquiver of $\underline{\mu}_{k-1} \circ \dots \circ \underline{\mu}_1 \circ \underline{\mu}_0(\hat{Q})$ of the form shown in Figure 19 (resp. Figure 20) where the vertices $z_k = x(0), x(1), \dots, x(d-1), \text{tr}(x(d))$, and $\text{tr}(y_k)$ (resp. $z_k = x(0), x(1), \dots, x(d-1)$, and $\text{tr}(y_k)$) are those appearing in the mutation sequence $\underline{\mu}_{A(k)} \circ \underline{\mu}_{B(k)} \circ \underline{\mu}_{C(k)}$ and the integers m_1, m_2, \dots, m_d are those defined by T_k in Definition 6.1. Recall that we only mutate at $\text{tr}(x(d))$ if $x(d) \neq x_1$. Furthermore, the ice quiver \bar{R}_k has the following properties:

- \bar{R}_k includes every frozen vertex that is connected to a mutable vertex appearing in Figure 19 (resp. Figure 20) by at least one arrow in $\underline{\mu}_{k-1} \circ \dots \circ \underline{\mu}_1 \circ \underline{\mu}_0(\hat{Q})$ where $\tilde{x}(1) := z'_{m_{d-1}}$, $\tilde{\text{tr}}(x(d)) := x'_{m_2}$, $\tilde{\text{tr}}(y_k) := x'_{m_1}$ and $\tilde{x}(s) := x'_{m_{d-s+2}}$ for⁴ $s \in [2, d-1]$ (resp. $\tilde{\text{tr}}(y_k) := x'_{m_1}$ and $\tilde{x}(s) := x'_{m_{d-s+1}}$ for⁵ $s \in [1, d-1]$),
- vertices y_m, y'_m, z_m , and z'_m appear in \bar{R}_k if and only if $\deg(y_k) = 4$ in Q ,
- vertices y_ℓ, y'_ℓ, z_ℓ , and z'_ℓ appear in \bar{R}_k if and only if $\deg(z_k) = 4$ in Q ,
- vertices y_t and y'_t appear in \bar{R}_k if and only if there exists a signed 3-cycle T_t in \mathcal{Q} with $k < t$ such that $\text{tr}|_{k,t}(y_t) = z_k$ and such that in $\underline{\mu}_{k-1} \circ \dots \circ \underline{\mu}_1 \circ \underline{\mu}_0(\hat{Q})$ the vertex x_t has been mutated exactly once⁶, and
- in Figure 19 (resp. Figure 20) $C_{1,k} := x_{m_{d-1}} \cdot \sigma_{k-1}^{-1}$, $\widetilde{C}_{1,k} := x'_{m_{d-1}}$, $C_{s,k} := y_{m_j} \cdot \sigma_{k-1}^{-1}$, and $\widetilde{C}_{s,k} := y'_{m_j}$ for $s \in [2, d]$ and $j = d-s+2$ (resp. $C_{s,k} := y_{m_j} \cdot \sigma_{k-1}^{-1}$ and $\widetilde{C}_{s,k} := y'_{m_j}$ for $s \in [1, d-1]$ and $j = d-s+2$).

Additionally, for each $k \in [n]$ we have $\underline{\mu}_k \circ \dots \circ \underline{\mu}_1 \circ \underline{\mu}_0(\widehat{\mathcal{Q}_{k,k}}) = \widetilde{\mathcal{Q}_{k,k}} \cdot \sigma_k$.

We will prove Lemma 7.2 in the case where the vertex $\text{tr}(x(d))$ appears in the mutation sequence $\underline{\mu}_k$ (i.e. when $x(d) \neq x_1$). Under this assumption, the following lemma will allow us to prove Lemma 7.2 inductively. The proof of Lemma 7.2 when $\text{tr}(x(d))$ does not appear in $\underline{\mu}_k$ is very similar so we omit it.

⁴If $d = 1$, then $\tilde{\text{tr}}(x(d)) = x'_{m_1} = x_k$.

⁵If $d = 1$, then $\tilde{\text{tr}}(x(d)) = x'_{m_1} = x_k$. Furthermore, $d = 1$, in this case, if and only if $k = 1$.

⁶Note that this can only happen if there exists $j < k$ such that $z_j = x_t$ and $x(d, k) = y_j$ as in Definition 6.1.

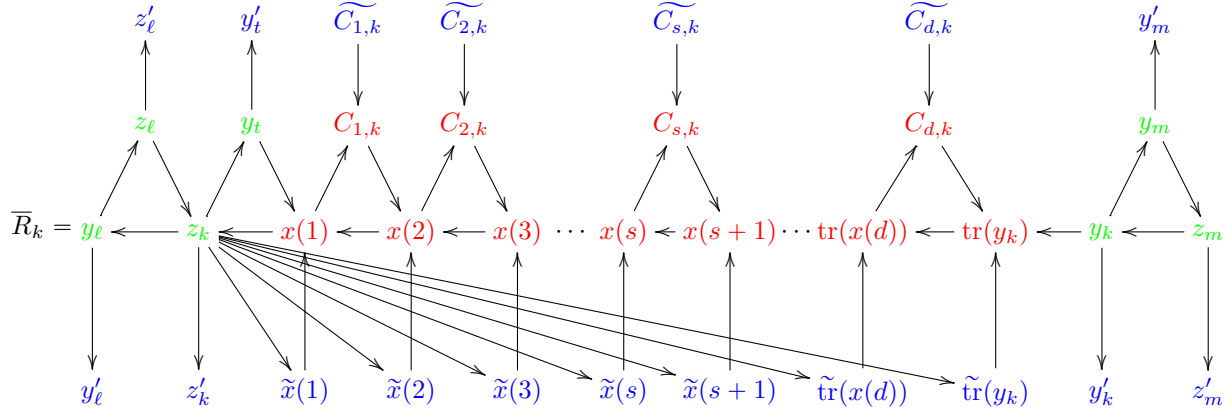


FIGURE 19. The local configuration around y_k and z_k just before μ_k is applied.

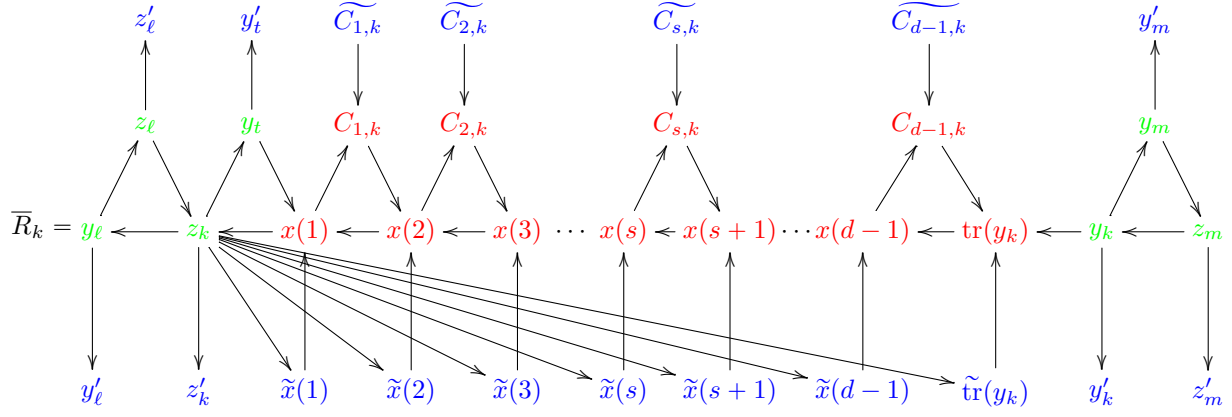


FIGURE 20. The local configuration in the special case when $x(d) = x_1$ since $\text{tr}(x_1)$ is not defined.

Lemma 7.3. Let $k \in [n]$ be given and let \bar{R}_k be the ice quiver described in Lemma 7.2. (See Figure 19.) Then

- $\mu_k(\bar{R}_k)$ has the form shown in Figure 22 (here, the vertices $y_m, y'_m, z_m, z'_m, y_\ell, y'_\ell, z_\ell, z'_\ell, y_t$, and y'_t appear in $\mu_k(\bar{R}_k)$ if and only if they appear in \bar{R}_k),
- $\mu_k(\bar{R}_k)$ is a full subquiver of $\mu_k \circ \dots \circ \mu_1 \circ \mu_0(\hat{Q})$,
- as one mutates \bar{R}_k along μ_k , one does so only at green vertices,
- $\mu_k(\bar{R}_k)$ includes every frozen vertex that is connected to a mutable vertex appearing in Figure 22 by at least one arrow in $\mu_k \circ \dots \circ \mu_1 \circ \mu_0(\hat{Q})$,
- the full subquiver of $\mu_{k-1} \circ \dots \circ \mu_1 \circ \mu_0(\hat{Q})$ on the vertices $(\hat{Q})_0 \setminus (\bar{R}_k)_0$ is unchanged by the mutation sequence μ_k .
- the vertices z_ℓ and z_m (rather than z_k) are the only mutable vertices in $\mu_k(\bar{R}_k)$ that are incident to multiple frozen vertices.

Additionally, for each $k \in [n]$, the full subquiver of $\mu_k \circ \dots \circ \mu_1 \circ \mu_0(\hat{Q})$ restricted to the green mutable vertices outside of $(\bar{R}_k)_0$, as well as the incident frozen vertices, equals the original framed quiver \hat{Q} restricted to those vertices.

Proof of Theorem 6.5. By the third assertion in Lemma 7.3, the associated mutation sequence $\underline{\mu} = \mu_n \circ \dots \circ \mu_1 \circ \mu_0$ of \mathcal{Q} is a green mutation sequence of \mathcal{Q} . By Lemma 7.2,

$$\mu_n \circ \dots \circ \mu_1 \circ \mu_0(\hat{Q}) = \mu_n \circ \dots \circ \mu_1 \circ \mu_0(\hat{Q}_{n,n}) = \check{Q}_{n,n} \cdot \sigma_n = \check{Q} \cdot \sigma_n$$

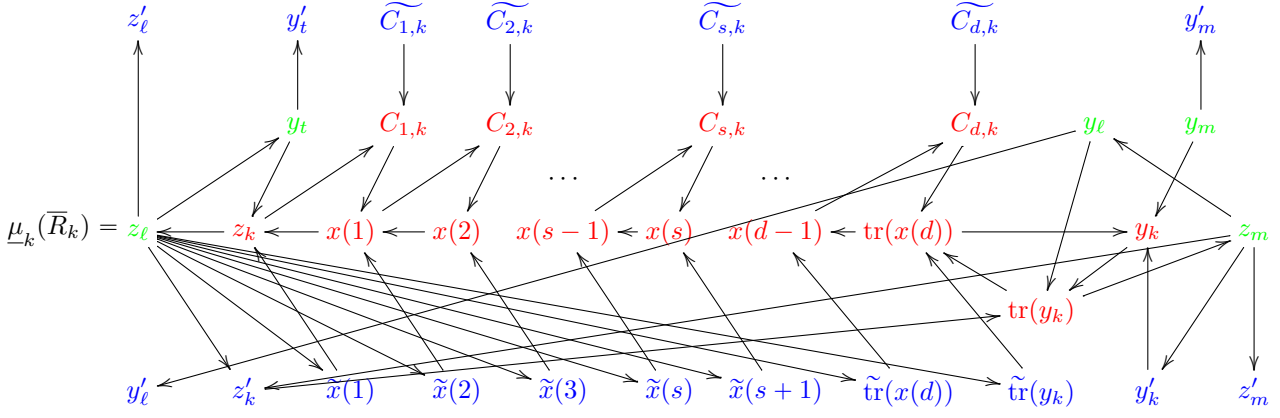


FIGURE 21. The quiver $\mu_k(\bar{R}_k)$ before rearrangement.

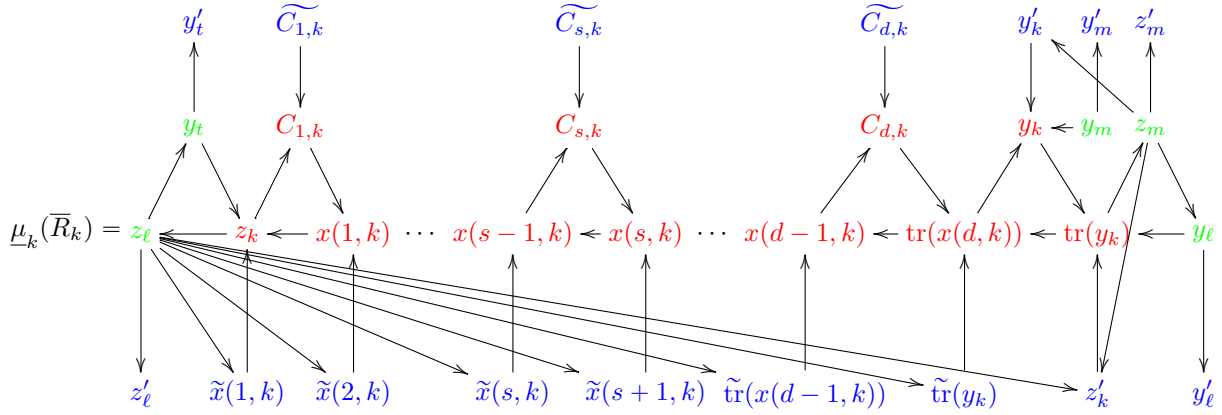


FIGURE 22. The quiver $\mu_k(\bar{R}_k)$ rearranged to look more like \bar{R}_{k+1} .

and so every mutable vertex of $\mu_n \circ \dots \circ \mu_1 \circ \mu_0(\hat{Q})$ is red. Thus $\underline{\mu} = \mu_n \circ \dots \circ \mu_1 \circ \mu_0 \in \text{green}(Q)$. \square

Remark 7.4. It follows from Lemma 5.1 that as one mutates \bar{R}_k along $\underline{\mu}_k = \mu_{i_r} \circ \dots \circ \mu_{i_1}$, we have that i_j in $\mu_{i_{j-1}} \circ \dots \circ \mu_{i_1}(\bar{R}_k)$ is incident to at most four other mutable vertices.

Proof of Lemma 7.3. The first assertion follows inductively by mutating the vertices of \bar{R}_k in the specified order $\underline{\mu}_k = \mu_{\text{tr}(y_k)} \circ \mu_{\text{tr}(x(d))} \circ \mu_{x(d-1)} \circ \mu_{x(d-2)} \circ \dots \circ \mu_{x(1)} \circ \mu_{x(0)} \circ \mu_{y_k}$, reading right-to-left. In particular, as this mutation sequence is applied to \bar{R}_k , Remark 7.4 shows that the mutable vertices incident to y_ℓ are located further and further to the right in Figure 19 until we see that they are $\text{tr}(y_k)$ and z_m at the end of the sequence. In fact, we observe after mutating \bar{R}_k at y_k that z_k is the unique green vertex of \bar{R}_k (with the exception of the vertices y_ℓ , z_ℓ , y_t , y_m and z_m , if they appear in \bar{R}_k). As we continue to mutate $\mu_{y_k}(\bar{R}_k)$ along the remaining mutations in $\underline{\mu}_k$, the unique green vertex is $x(s)$ for some $s \in [0, d-1]$ or as $\text{tr}(x(d))$ or $\text{tr}(y_k)$ (as before, with the exception of the vertices y_ℓ , z_ℓ , y_t , y_m and z_m). Iteratively mutating at this unique green vertex exactly corresponds to performing the mutation sequence $\underline{\mu}_{A(k)} \circ \underline{\mu}_{B(k)} \circ \underline{\mu}_{C(k)}$ on $\underline{\mu}_{D(k)}(\bar{R}_k)$.

The second assertion, $\mu_k(\bar{R}_k)$ is a full subquiver of $\underline{\mu}_k \circ \dots \circ \mu_1 \circ \mu_0(\hat{Q})$, follows since the vertices of Q at which one mutates when applying $\underline{\mu}_k$ are all vertices of \bar{R}_k . One can see that the third assertion follows from the above observation that a unique vertex becomes green as we iteratively mutate. The fourth assertion holds for $\mu_k(\bar{R}_k)$ since it holds for \bar{R}_k . The fifth assertion follows since the vertices in the support of $\underline{\mu}_k$ are all disconnected from the vertices in $(\underline{\mu}_{k-1} \circ \dots \circ \mu_1 \circ \mu_0(\hat{Q}))_0 \setminus (\bar{R}_k)_0$. Further, the sixth assertion is demonstrated inductively as

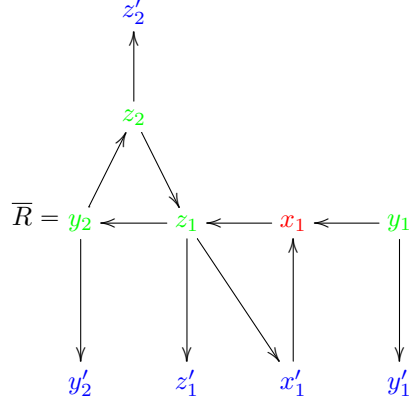


FIGURE 23. The subquiver $\bar{R} = \bar{R}_1$ of $\underline{\mu}_0(\hat{Q})$.

we mutate $x(s)$ for $s \in [0, d-1]$. Lastly, by restricting to the green mutable vertices outside of $(\bar{R}_k)_0$ and the incident frozen vertices, it is clear that the mutation sequence $\underline{\mu}_k$ leaves this full subquiver unaffected. \square

Proof of Lemma 7.2. We prove the lemma by induction. For $k = 1$, observe that $\underline{\mu}_0(\hat{Q})$ has the full subquiver \bar{R} shown in Figure 23 where we assume that $n > 1$. We show that \bar{R} has all of the properties that \bar{R}_1 must satisfy. Note that $\text{tr}(y_1) = x_1$ and for $k = 1$ one has that $x(1) = x_{m_1} = x_1$. Since $\deg(y_1) = 2$, no vertices y_m, y'_m, z_m , and z'_m appear in \bar{R} , as desired. Since only vertex x_1 has been mutated to obtain $\underline{\mu}_0(\hat{Q})$, no arrows between vertices of a signed 3-cycle T_t with $1 < t$ and vertices of signed 3-cycle T_i with $i \leq 1$ have been created. Furthermore, there is no signed 3-cycle T_t of \mathcal{Q} with $1 < t$ where $\text{tr}|_{1,t}(y_t) = z_1$. Note that in this degenerate case, $\text{tr}(y_1) = x(1)$ and so no $C_{i,1}$'s or $\widetilde{C}_{i,1}$'s appear in \bar{R}_1 , and $\tilde{x}(1) = \tilde{\text{tr}}(y_1) = x'_1$. Thus the quiver \bar{R} satisfies all of the properties that \bar{R}_1 must satisfy. Further, in this special case $\widehat{\mathcal{Q}}_{0,0}$ contains only the vertex x_1 and x'_1 and σ_0 is the identity permutation. Thus $\underline{\mu}_0 \widehat{\mathcal{Q}}_{0,0}$ indeed equals $\widehat{\mathcal{Q}}_{0,0} \cdot \sigma_0$.

Now assume that $k > 1$ and that $\underline{\mu}_{k-1} \circ \dots \circ \underline{\mu}_1 \circ \underline{\mu}_0(\hat{Q})$ has a full subquiver \bar{R}_k with the properties in the statement of the lemma. To show that $\underline{\mu}_k \circ \dots \circ \underline{\mu}_1 \circ \underline{\mu}_0(\hat{Q})$ has the desired full subquiver \bar{R}_{k+1} , we consider four cases:

- i) $\deg(y_k) = 2$ and $\deg(z_k) = 4$,
- ii) $\deg(y_k) = 4$ and $\deg(z_k) = 2$,
- iii) $\deg(y_k) = 4$ and $\deg(z_k) = 4$, and
- iv) $\deg(y_k) = 2$ and $\deg(z_k) = 2$.

Suppose that we are in Case i). By the properties of the ice quiver \bar{R}_k , this means that vertices y_m, y'_m, z_m , and z'_m do not appear in \bar{R}_k . This also implies that $\ell = k + 1$. Now Lemma 7.3 implies that $\underline{\mu}_k(\bar{R}_k)$ has the form shown in Figure 24 where the vertices y_t and y'_t appear $\underline{\mu}_k(\bar{R}_k)$ if and only if they appear in \bar{R}_k . Note that the quiver in Figure 24 is the same as the quiver in Figure 22 with the notation updated accordingly. In particular, the integers $m_1^{(k+1)}, m_2^{(k+1)}, \dots, m_{d+1}^{(k+1)} \in [n]$ and the vertices $x(1, k+1), \dots, x(d+1, k+1) \in (Q)_0$ are those defined by T_{k+1} following Definition 6.1. Since the signed 3-cycles T_k and T_{k+1} share the vertex z_k (i.e. $z_k = x_{k+1}$), we have that

$$(3) \quad m_1^{(k+1)} = k+1, m_2^{(k+1)} = m_1, \dots, m_j^{(k+1)} = m_{j-1}, \dots, m_{d+1}^{(k+1)} = m_d$$

and

$$x(1, k+1) = z_k, x(2, k+1) = x(1), \dots, x(s, k+1) = x(s-1), \dots, x(d+1, k+1) = x(d).$$

This implies that $\text{tr}(x(d+1, k+1)) = \text{tr}(x(d, k))$ and $\text{tr}(y_{k+1}) = \text{tr}(y_k)$. Now we also obtain that

$$\tilde{x}(1, k+1) = z'_{m_{d+1}^{(k+1)}-1} = z'_{m_d-1} = \tilde{x}(1, k) \text{ and } \tilde{x}(s, k+1) = x'_{m_{d+1}^{(k+1)}-s+2} = x'_{m_j^{(k+1)}} = x'_{m_{j-1}} = \tilde{x}(s, k)$$

for $s \in [2, d]$ where $j = (d+1) - s + 2$ and that

$$\tilde{\text{tr}}(x(d+1, k+1)) = x'_{m_2^{(k+1)}} = x'_{m_1} = \tilde{\text{tr}}(y_k) \text{ and } \tilde{\text{tr}}(y_{k+1}) = x'_{m_1^{(k+1)}} = x'_{k+1} = z'_k$$

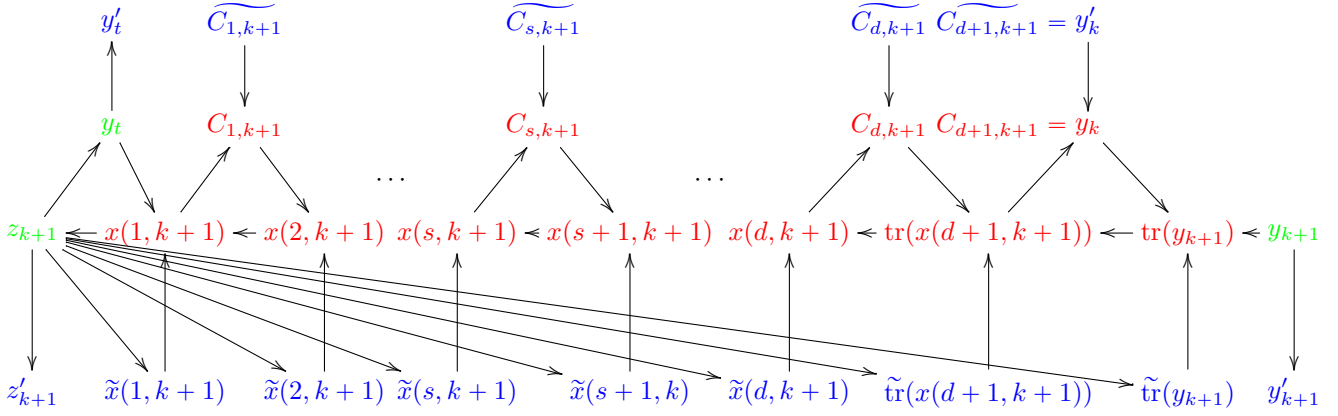


FIGURE 24. The quiver $\mu_k(\bar{R}_k)$ obtained by mutating \bar{R}_k in Case i).

where the last equality follows from the fact that T_k and T_{k+1} share the vertex z_k . Thus we have labeled the vertices of $\mu_k(\bar{R}_k)$ accordingly in Figure 24. Furthermore, that the signed 3-cycles T_k and T_{k+1} share the vertex z_k implies that $z_{k+1} = \text{tr}|_{k+1,t}(y_t)$ if and only if $z_k = \text{tr}|_{k,t}(y_t)$.

Next, observe that for any $s \in [d]$ we have $C_{s,k} \cdot \tau_k^{-1} = C_{s,k}$ since we do not mutate $C_{s,k}$ when applying μ_k . Additionally $x_{m_{d+1}-1}^{(k+1)} = x_{m_d-1}$ and $y_{m_{j+1}}^{(k+1)} = y_{m_j}$ (for $j = (d+1) - s + 2$ where $s \in [2, d]$) follows from (3). Comparing with the fifth bullet point of Lemma 7.2, we obtain $C_{s,k} = C_{s,k} \cdot \tau_k^{-1} = C_{s,k+1}$ and $\widetilde{C_{s,k}} = \widetilde{C_{s,k}} \cdot \tau_k^{-1} = \widetilde{C_{s,k+1}}$ for any $s \in [d]$.

Now let $C_{d+1,k+1} = y_k$ and $\widetilde{C_{d+1,k+1}} = y'_k$. Note that $y_k \cdot \sigma_{k-1}^{-1} = y_k$ since y_k has not been mutated in $\mu_{k-1} \circ \dots \circ \mu_0(\hat{Q})$. Furthermore, $y_k \cdot \sigma_{k-1}^{-1} \tau_k^{-1} = y_k \cdot \tau_k^{-1} = y_k$ by the definition of τ_k so $C_{d+1,k+1} = y_k \cdot \sigma_k^{-1}$, as desired.

We now construct an ice quiver \bar{R} that is the full subquiver of $\mu_k \circ \dots \circ \mu_1 \circ \mu_0(\hat{Q})$ on the vertices of $\mu_k(\bar{R}_k)$, as well as the vertices x_r, y_r, z_r and corresponding frozen vertices x'_r, y'_r, z'_r of any signed 3-cycles T_r of \hat{Q} where $k < r$ and z_{k+1} or y_{k+1} is a vertex of T_r . Comparing this construction of \bar{R} to the quiver \bar{R}_{k+1} appearing in Figure 19, we verify that \bar{R} indeed equals \bar{R}_{k+1} and satisfies the five properties listed as bullet points in Lemma 7.2.

Next, suppose that we are in Case ii). In this situation, we have that $m = k+1$ and the vertices y_ℓ, y'_ℓ, z_ℓ , and z'_ℓ do not belong to \bar{R}_k . Now Lemma 7.3 implies that $\mu_k(\bar{R}_k)$ has the form shown in Figure 25. We let T_p (resp. T_q) be the signed 3-cycle not equal to T_{k+1} that contains z_{k+1} (resp. y_{k+1}), if they exist. Define \bar{R} to be the ice quiver that is a full subquiver of $\mu_k \circ \dots \circ \mu_1 \circ \mu_0(\hat{Q})$ on the vertices

$$y_{k+1}, y'_{k+1}, z_{k+1}, z'_{k+1}, \text{tr}(y_k), z'_k, y_k, y'_k, \text{tr}(x(d)), x'_k, y_p, y'_p, z_p, z'_p, y_q, y'_q, z_q, z'_q$$

where we include y_p and y'_p (resp. $z_p, z'_p, y_q, y'_q, z_q$, and z'_q) in \bar{R} if and only if y_p and y'_p (resp. $z_q, z'_q, y_q, y'_q, z_q$, and z'_q) appear in $\mu_k(\bar{R}_k)$, i.e. depending on if $\deg(y_{k+1}) = 4$ and if $\deg(z_{k+1}) = 4$. See Figure 26.

Just as above, we claim that the ice quiver \bar{R} equals \bar{R}_{k+1} and satisfies the five bullet points in the statement of Lemma 7.2. It is easy to see that \bar{R} is a full subquiver of $\mu_k \circ \dots \circ \mu_1 \circ \mu_0(\hat{Q})$ that includes every frozen vertex that is connected to a mutable vertex appearing in Figure 26 by at least one arrow in $\mu_k \circ \dots \circ \mu_1 \circ \mu_0(\hat{Q})$. In particular, $\mu_k(\bar{R}_k)$ has this property and no vertices of T_p or T_q and neither y_{k+1} nor z_{k+1} have been mutated in $\mu_k \circ \dots \circ \mu_1 \circ \mu_0(\hat{Q})$. Furthermore, defining $m_1^{(k+1)} \in [n]$, $x(0, k+1)$, and $x(1, k+1) \in (\hat{Q})_0$ just as we did in Case i), following Definition 6.1, and using the fact that $\text{sgn}(T_{k+1}) = +$, we have $m_1^{(k+1)} = k+1$, $x(0, k+1) = z_{k+1}$, and $x(1, k+1) = x_{k+1}$. Hence we obtain that

$$\text{tr}(x(1, k+1)) = \text{tr}(x_{k+1}) = \text{tr}(y_k) \text{ and } z'_{m_1^{(k+1)}-1} = z'_k,$$

as desired. Additionally, the fact that $\text{sgn}(T_{k+1}) = +$ also implies that

$$\text{tr}(y_{k+1}) = x_{k+1} = y_k \text{ and } x'_{m_1^{(k+1)}} = x'_k = y'_k,$$

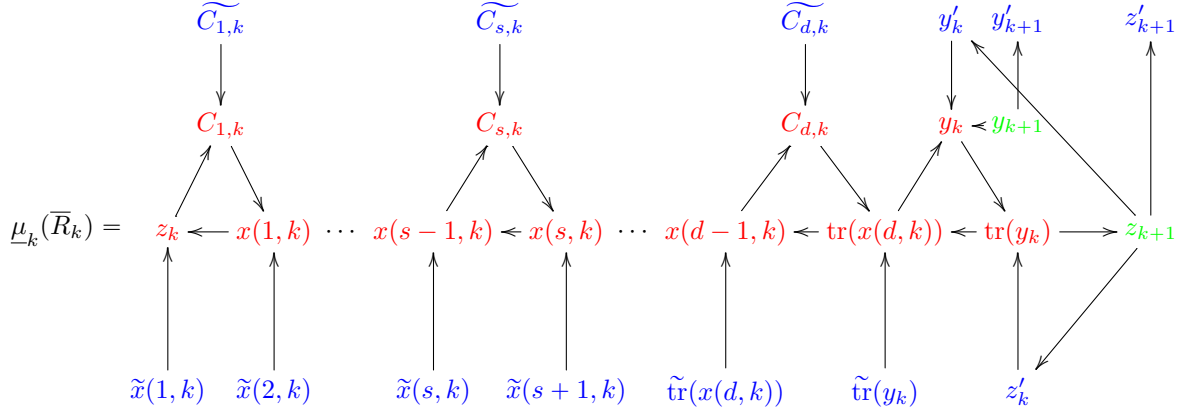


FIGURE 25. The quiver obtained by mutating \bar{R}_k in Case ii).

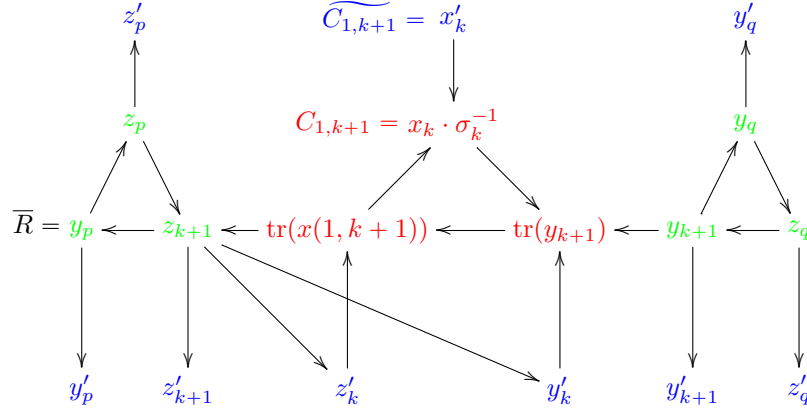


FIGURE 26. The quiver $\bar{R} = \bar{R}_{k+1}$ that we obtain in Case ii).

as desired. These calculations are reflected in the quiver \bar{R} shown in Figure 26, thus verifying the first three bullet points of Lemma 7.2.

Furthermore, since $\deg(z_k) = 2$, there is no signed 3-cycle T_t with $k+1 < t$ such that $\text{tr}|_{k+1,t}(y_t) = z_{k+1}$ in $\underline{\mu}_k \circ \dots \circ \underline{\mu}_1 \circ \underline{\mu}_0(\hat{Q})$ vertex x_t has been mutated exactly once. The fourth bullet point follows. Now observe that $\text{tr}(y_k) = x'_{m_1} = x'_k$. Since we have applied a maximal green sequence to \mathcal{Q}_k and since $\text{tr}(x(d, k))$ is only connected to the frozen vertex x'_k , Proposition 2.10 of [5] implies that $\text{tr}(x(d, k)) = x_k \cdot \sigma_k^{-1}$. We thus have the fifth bullet point.

Case iii) is similar to Case ii), but with some key differences. In this situation, we again have that $m = k+1$ but this time both y_ℓ and z_ℓ are relevant. Now Lemma 7.3 implies that $\underline{\mu}_k(\bar{R}_k)$ has the form shown in Figure 27. We let T_p (resp. T_q) be the signed 3-cycles incident to z_{k+1} (resp. y_{k+1}) if they exist. Define \bar{R} to be the ice quiver that is a full subquiver of $\underline{\mu}_k \circ \dots \circ \underline{\mu}_1 \circ \underline{\mu}_0(\hat{Q})$ on the vertices

$$y_{k+1}, y'_{k+1}, z_{k+1}, z'_{k+1}, \text{tr}(y_k), z'_k, y_k, y'_k, \text{tr}(x(d)), x'_k, y_\ell, y'_\ell, y_p, y'_p, z_p, z'_p, y_q, y'_q, z_q, z'_q$$

where we include y_p and y'_p (resp. $z_p, z'_p, y_q, y'_q, z_q$, and z'_q) in \bar{R} if and only if y_p and y'_p (resp. $z_q, z'_q, y_q, y'_q, z_q$, and z'_q) appear in $\underline{\mu}_k(\bar{R}_k)$, i.e. depending on if $\deg(y_{k+1}) = 4$ and if $\deg(z_{k+1}) = 4$. See Figure 28.

We claim that the ice quiver \bar{R} has the properties in the statement of Lemma 7.2. It is easy to see that \bar{R} is a full subquiver of $\underline{\mu}_k \circ \dots \circ \underline{\mu}_1 \circ \underline{\mu}_0(\hat{Q})$. That \bar{R} includes every frozen vertex that is connected to a mutable vertex appearing in Figure 28 by at least one arrow in $\underline{\mu}_k \circ \dots \circ \underline{\mu}_1 \circ \underline{\mu}_0(\hat{Q})$ follows from the fact that $\underline{\mu}_k(\bar{R}_k)$ has this property and from the fact that no vertices of T_p or T_q and neither y_{k+1} nor z_{k+1} have been mutated in

$\underline{\mu}_k \circ \cdots \circ \underline{\mu}_1 \circ \underline{\mu}_0(\hat{Q})$. Now observe that $\tilde{\text{tr}}(y_k) = x'_{m_1} = x'_k$. As in Case ii), Proposition 2.10 of [5] implies that $\text{tr}(x(d, k)) = x_k \cdot \sigma_k^{-1}$.

Let $m_1^{(k+1)} \in [n]$ be the integer from the definition of $\underline{\mu}_{k+1}$, and let $x(0, k+1), x(1, k+1) \in (Q)_0$ be the vertices from the definition of $\underline{\mu}_{k+1}$. As in Case ii), we are using the fact that $\text{sgn}(T_{k+1}) = +$. Now notice that $m_1^{(k+1)} = m_d^{(k+1)} = k+1$, $x(0, k+1) = z_{k+1}$, and $x(1, k+1) = x_{k+1}$. We now obtain that

$$\text{tr}(x(d, k+1)) = \text{tr}(x_{k+1}) = \text{tr}(y_k),$$

as desired. The fact that $\text{sgn}(T_{k+1}) = +$ implies that

$$\text{tr}(y_{k+1}) = x_{k+1} = y_k.$$

Since $\deg(z_{k+1}) = 4$, the vertices y_ℓ and y'_ℓ both appear in \bar{R} . Now it is clear that $\deg(z_{k+1}) = 4$ if and only if $\text{tr}|_{k+1, \ell}(y_\ell) = z_{k+1}$ and the signed 3-cycle T_ℓ has the property that vertex x_ℓ has been mutated exactly once in $\underline{\mu}_k \circ \cdots \circ \underline{\mu}_1 \circ \underline{\mu}_0(\hat{Q})$. Hence we see that the vertex y_ℓ is positioned in \bar{R} exactly where y_t is positioned in \bar{R}_{k+1} , see Figure 19. These calculations are reflected in the quiver \bar{R} shown in Figure 28, and we see that this quiver has the properties that the desired quiver \bar{R}_{k+1} should have. The proof of the five bullet points of Lemma 7.2 in Case iii) concludes in the same way as the proof for Case ii).

In addition, we illustrate how in Case iii), for each $c \in [n]$ satisfying $k < c \leq \ell$ there is an ice quiver $\bar{R}_{c, \ell}$ that is isomorphic to \bar{R}_ℓ and that appears as a full subquiver of $\underline{\mu}_{c-1} \circ \cdots \circ \underline{\mu}_1 \circ \underline{\mu}_0(\hat{Q})$. Furthermore, we show that $\bar{R}_{\ell, \ell} = \bar{R}_\ell$. This analysis will be used in the argument for Case iv), which is given below.

As we are in Case iii), we know that both vertices y_k and z_k are of degree 4 and the signed 3-cycles T_k, T_{k+1} , and T_ℓ appear in a full subquiver of \mathcal{Q} of the form shown in Figure 29 or 30. It follows that y_ℓ and z_ℓ , which are incident to z_k in $\underline{\mu}_{k-1} \circ \cdots \circ \underline{\mu}_1 \circ \underline{\mu}_0(\hat{Q})$, will not be mutated until after applying the mutation sequences $\underline{\mu}_k, \underline{\mu}_{k+1}, \dots, \underline{\mu}_r$ where $k \leq r < \ell$ (see Figure 31). To be precise, the quiver in Figure 31 is a full subquiver of $\underline{\mu}_{k-1} \circ \cdots \circ \underline{\mu}_1 \circ \underline{\mu}_0(\hat{Q})$, which we define as follows. Letting $k < r < \ell$ be the integer such that $z_r = \text{tr}(y_\ell)$ and e such that $x(e, r) = x_{k+1} = y_k$, this full subquiver includes the vertices of \bar{R}_{k-1} as well as the mutable vertices of the signed 3-cycles $T_{m_e^{(r)}} = T_{k+1}, T_{m_{e-1}^{(r)}}, \dots, T_{m_2^{(r)}}, T_{m_1^{(r)}} = T_r$, as in Definition 6.1, and their corresponding frozen vertices.

We now mutate the quiver shown in Figure 31 along $\underline{\mu}_k$. By Lemma 7.3, this does not affect the full subquiver of $\underline{\mu}_{k-1} \circ \cdots \circ \underline{\mu}_1 \circ \underline{\mu}_0(\hat{Q})$ on the vertices $(\hat{Q})_0 \setminus (\bar{R}_k)_0$. Thus we conclude that $\underline{\mu}_k \circ \cdots \circ \underline{\mu}_1 \circ \underline{\mu}_0(\hat{Q})$ has the quiver shown in Figure 32 as a full subquiver. We observe that the permutation σ_{k-1}^{-1} has the vertices y_k and z_k as fixed points. However, τ_k^{-1} maps $z_k \mapsto \text{tr}(y_k)$ and fixes y_k . These equalities are illustrated in Figure 32.

Next, we relabel the vertices of the quiver in Figure 32 to obtain the quiver shown in Figure 33. In particular, since $\text{sgn}(T_\ell) = -$ with $x_\ell = z_k$, note that $z_k = x(1, \ell)$, $x(s, k) = x(s+1, \ell)$, and $\text{tr}(y_k) = \text{tr}|_{k, \ell}(y_\ell)$. Define $\bar{R}_{k+1, \ell}$ to be the full subquiver of $\underline{\mu}_k \circ \cdots \circ \underline{\mu}_1 \circ \underline{\mu}_0(\hat{Q})$ on the red vertices appearing in Figure 33, the neighbors of y_ℓ and z_ℓ , as well as the frozen vertices to which these all are connected. One observes that $\bar{R}_{k+1, \ell}$ and \bar{R}_ℓ are isomorphic as ice quivers. Furthermore, we will see that $\bar{R}_{k+1, \ell}$ has the same vertices as \bar{R}_ℓ with the exceptions of y_k and $\text{tr}|_{k, \ell}(y_\ell)$.

For $k < c \leq \ell$, we define $\bar{R}_{c, \ell}$ analogously as the full subquiver of $\underline{\mu}_{c-1} \circ \cdots \circ \underline{\mu}_1 \circ \underline{\mu}_0(\hat{Q})$ on the set of vertices $(\bar{R}_{k+1, \ell})_0 \cdot \tau_{k+1}^{-1} \tau_{k+2}^{-1} \cdots \tau_{c-1}^{-1}$. With this definition, we observe that $\bar{R}_{c+1, \ell}$ is identical to $\bar{R}_{c, \ell}$ except possibly at two vertices. In particular, for $k < c \leq \ell$, if T_c does not appear in Figure 29 (resp. Figure 30), then the mutation sequence $\underline{\mu}_c$ does not involve any vertices that appear in $\bar{R}_{c, \ell}$. Consequently, after mutation by $\underline{\mu}_c$, we obtain $\bar{R}_{c+1, \ell} = \bar{R}_{c, \ell}$.

On the other hand, when T_c , for $k < c \leq \ell$, i.e. $c = m_s^{(r)}$ for some s , does appear in Figure 29 (resp. Figure 30), then the mutation sequence $\underline{\mu}_c$, as indicated by bold arrows in Figures 33 and 34, involves vertices $y_k \cdot \sigma_{c-1}^{-1}$ and $z_k \cdot \sigma_{c-1}^{-1}$. In this case, $\bar{R}_{c+1, \ell} \cong \bar{R}_{c, \ell}$ with the relabeling $y_k \cdot \sigma_{c-1}^{-1} \mapsto y_k \cdot \sigma_c^{-1}$ and $z_k \cdot \sigma_{c-1}^{-1} \mapsto z_k \cdot \sigma_c^{-1}$ since each application of $\underline{\mu}_c$ permutes these two vertices by τ_c^{-1} . This isomorphism of full subquivers follows from Lemma 7.3.

We obtain the identity $z_k \cdot \sigma_c^{-1} = \text{tr}|_{m_s^{(r)}, \ell}(y_\ell)$ for $m_s^{(r)} \leq c < m_{s-1}^{(r)}$ when $s \in [2, e]$ or $r = m_1^{(r)} \leq c < \ell$ when $s = 1$, which is implicit in Figure 34, by Lemma 7.5. We leave this argument until after completing the proof of Lemma 7.2 (see below). We also observe, by the specialization $c = \ell - 1$, that $y_k \cdot \sigma_{\ell-1}^{-1} = C_{d+1, \ell}$ and

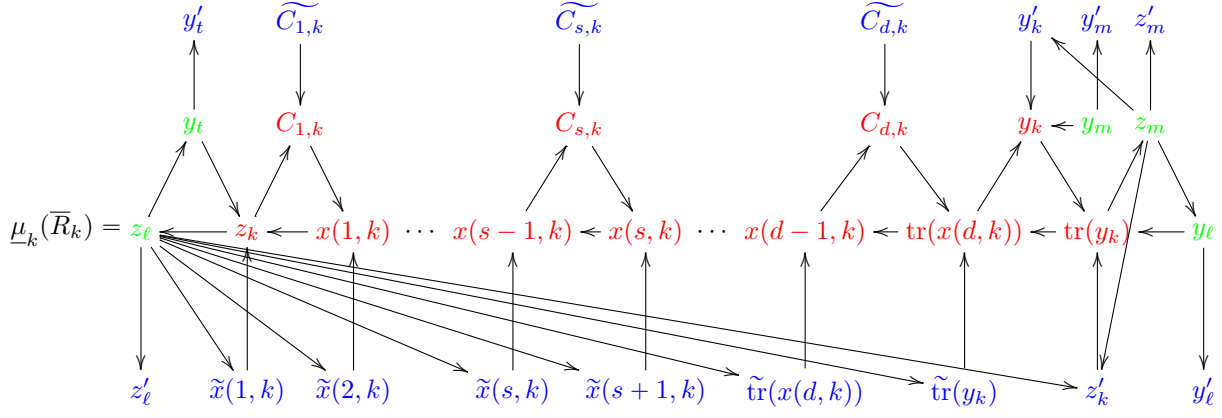


FIGURE 27. The quiver obtained by mutating \bar{R}_k in Case iii).

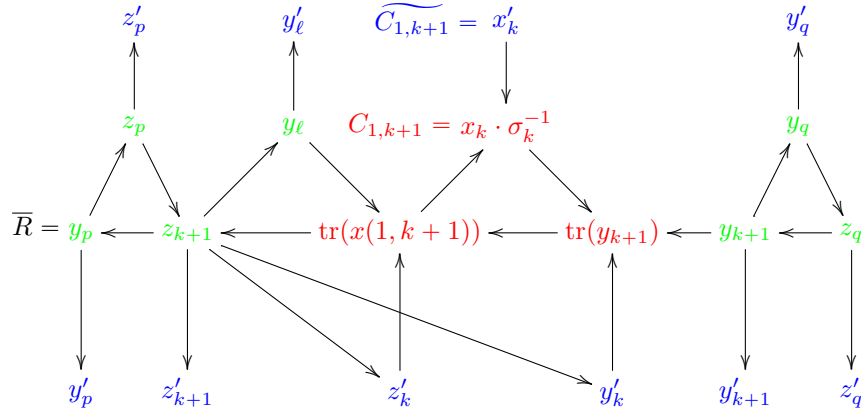


FIGURE 28. The quiver $\bar{R} = \bar{R}_{k+1}$ that we obtain in Case iii).

$z_k \cdot \sigma_{\ell-1}^{-1} = \text{tr}(y_\ell)$. Consequently, we eventually arrive at the configuration in Figure 35 with configurations of the form as in Figure 34 as intermediate steps. In summary, we conclude that $\bar{R}_{\ell,\ell} = \bar{R}_\ell$ as desired.

Next, suppose we are in Case iv). Since $\deg(z_k) = 2$, this case is similar to Case i). However, here we have $\deg(y_k) = 2$ as well, and so the quiver $\mu_k(\bar{R}_k)$ looks like Figure 22, but without $y_\ell, y'_\ell, z_\ell, z'_\ell, y_m, y'_m, z_m$, nor z'_m . The green vertex y_t and y'_t may or may not appear in the quiver $\mu_k(\bar{R}_k)$. In the latter case, $k = n$ and we have applied the entire mutation sequence μ to \hat{Q} . In the former case, we see that $t = k + 1$, and T_t can be realized as a signed 3-cycle T_ℓ appearing in one of Figures 29 or 30. Now by the argument at the end of Case iii), $\bar{R}_{t,t} = \bar{R}_t$ is indeed a full subquiver of Figure 35 with the desired properties. The five bullet points of Lemma 7.2 follow immediately.

Lastly, for all four cases, we wish to describe the quiver obtained by $\mu_k \circ \dots \circ \mu_1 \circ \mu_0(\widehat{\mathcal{Q}_{k,k}})$. To this end, we decompose the vertices of $\widehat{\mathcal{Q}_{k,k}}$ into two sets: (1) $(\widehat{\mathcal{Q}_{k,k}})_0 \setminus (\bar{R}_k)_0$ and (2) $(\bar{R}_k)_0 \cap (\widehat{\mathcal{Q}_{k,k}})_0$. By induction, we have

$$\mu_{k-1} \circ \dots \circ \mu_1 \circ \mu_0(\widehat{\mathcal{Q}_{k-1,k-1}}) = \widetilde{\mathcal{Q}_{k-1,k-1}} \cdot \sigma_{k-1}$$

and we observe that $(\widehat{\mathcal{Q}_{k,k}})_0 \setminus (\bar{R}_k)_0 \subset (\widehat{\mathcal{Q}_{k-1,k-1}})_0$. The fifth bullet point of Lemma 7.3 implies that the quiver $\mu_{k-1} \circ \dots \circ \mu_1 \circ \mu_0(\widehat{\mathcal{Q}_{k,k}}|_{(\widehat{\mathcal{Q}_{k,k}})_0 \setminus (\bar{R}_k)_0})$ ⁷ is unchanged by the mutation sequence μ_k , and the permutation τ_k fixes

⁷We define $\widehat{\mathcal{Q}_{k,k}}|_{(\widehat{\mathcal{Q}_{k,k}})_0 \setminus (\bar{R}_k)_0}$ (resp. $\widetilde{\mathcal{Q}_{k,k}}|_{(\widehat{\mathcal{Q}_{k,k}})_0 \setminus (\bar{R}_k)_0}$) to be the ice quiver that is a full subquiver of $\widehat{\mathcal{Q}_{k,k}}$ (resp. $\widetilde{\mathcal{Q}_{k,k}}$) on the vertices of $(\widehat{\mathcal{Q}_{k,k}})_0 \setminus (\bar{R}_k)_0$.

all vertices in $(\widehat{\mathcal{Q}_{k,k}})_0 \setminus (\overline{R}_k)_0$. It follows that

$$\underline{\mu}_k \circ \cdots \circ \underline{\mu}_1 \circ \underline{\mu}_0 \left(\widehat{\mathcal{Q}_{k,k}}|_{(\widehat{\mathcal{Q}_{k,k}})_0 \setminus (\overline{R}_k)_0} \right) = \left(\widetilde{\mathcal{Q}_{k,k}}|_{(\widehat{\mathcal{Q}_{k,k}})_0 \setminus (\overline{R}_k)_0} \right) \cdot \sigma_k.$$

Additionally, the first bullet point of Lemma 7.3 indicates how the vertices of the second set, i.e. $(\overline{R}_k)_0 \cap (\widehat{\mathcal{Q}_{k,k}})_0$, are affected by $\underline{\mu}_k$. Comparing Figures 19 and 21, we see that the vertices of \overline{R}_k have been permuted cyclically exactly as described by τ_k . We conclude that

$$\underline{\mu}_k \circ \cdots \circ \underline{\mu}_1 \circ \underline{\mu}_0 (\widehat{\mathcal{Q}_{k,k}}) = \widetilde{\mathcal{Q}_{k,k}} \cdot \tau_k \sigma_{k-1} = \widetilde{\mathcal{Q}_{k,k}} \cdot \sigma_k$$

which completes the proof of Lemma 7.2. \square

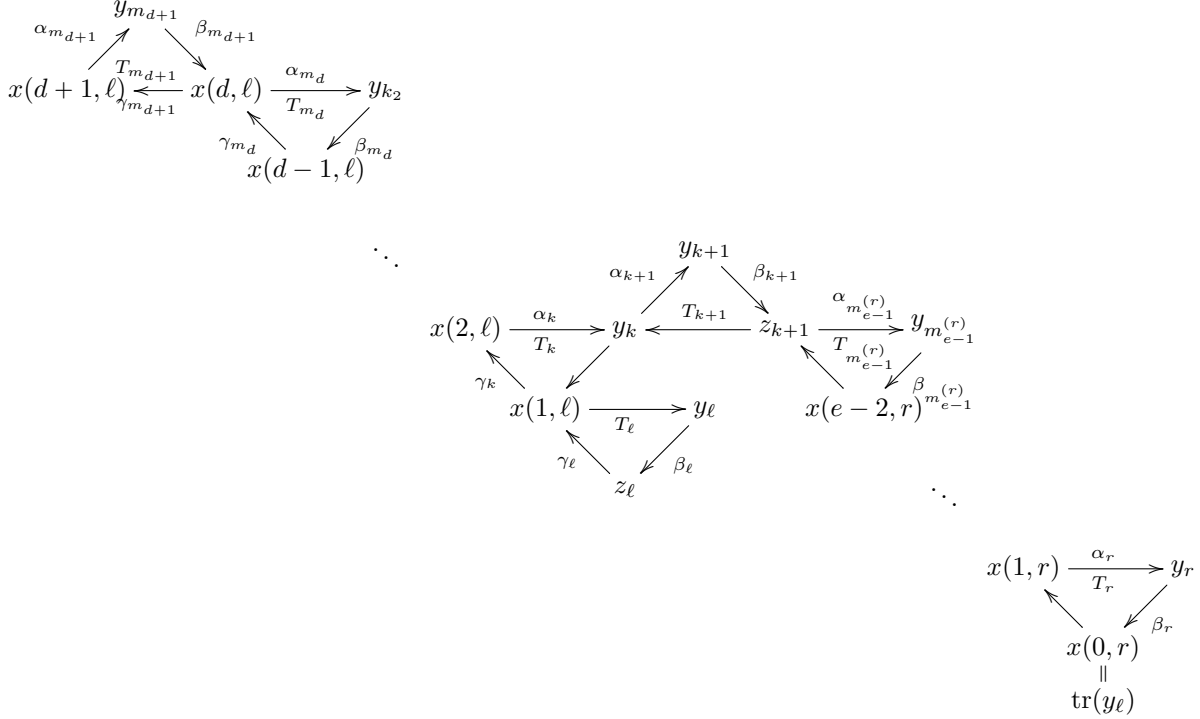


FIGURE 29. A full subquiver of \mathcal{Q} showing one possible configuration of the signed 3-cycles T_k , T_{k+1} , and T_ℓ , as described in the proof of Lemma 7.2 at the end of Case iii).

Lemma 7.5. Using the notation from the proof of Lemma 7.2, for any $s \in [2, e]$ and any $c \in [n]$ satisfying $m_s^{(r)} \leq c < m_{s-1}^{(r)}$, one has $z_k \cdot \sigma_c^{-1} = \text{tr}|_{m_s^{(r)}, \ell}(y_\ell)$ (see Figure 34). Additionally, for any $c \in [n]$ satisfying $r = m_1^{(r)} \leq c < \ell$ we have $z_k \cdot \sigma_c^{-1} = \text{tr}(y_\ell)$.

Proof. For $c = k + 1$, we have

$$\begin{aligned} z_k \cdot \sigma_{k+1}^{-1} &= z_k \cdot \sigma_k^{-1} \tau_{k+1}^{-1} \\ &= \text{tr}(y_k) \cdot \tau_{k+1}^{-1} && \text{(see Figure 32)} \\ &= \text{tr}(x(1, k+1)) \cdot \tau_{k+1}^{-1} && \text{(using that } \text{sgn}(T_{k+1}) = + \text{)} \\ &= x(0, k+1) && \text{(by the definition of } \tau_{k+1} \text{)} \\ &= z_k && \text{(by Definition 6.1)} \\ &= \text{tr}|_{k+1, \ell}(y_\ell), && \text{(by Definition 6.2)} \end{aligned}$$

as desired. Now suppose that $z_k \cdot \sigma_c^{-1} = \text{tr}|_{m_s^{(r)}, \ell}(y_\ell)$ where $s \in [e]$ and $m_s^{(r)} \leq c < m_{s-1}^{(r)}$. Then for $c \in [n]$ satisfying $m_{s-1}^{(r)} \leq c < m_{s-2}^{(r)}$ we have

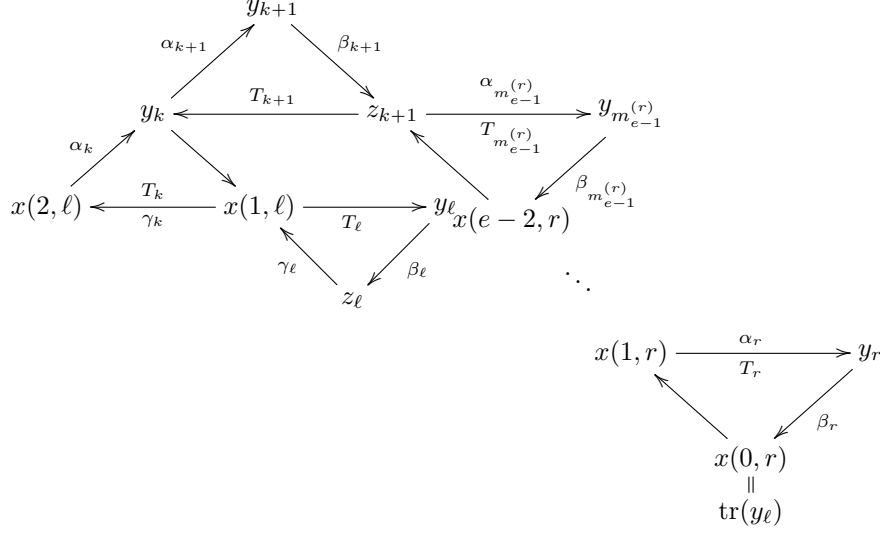


FIGURE 30. A full subquiver of \mathcal{Q} showing the other possible configuration of the signed 3-cycles T_k , T_{k+1} , and T_ℓ , as described in the proof of Lemma 7.2 at the end of Case iii).

$$\begin{aligned}
z_k \cdot \sigma_c^{-1} &= z_k \cdot \sigma_{m_{s-1}^{(r)}-1}^{-1} \tau_{m_{s-1}^{(r)}}^{-1} \cdots \tau_c^{-1} \\
&= \text{tr}|_{m_{s-1}^{(r)}, \ell}(y_\ell) \cdot \tau_{m_{s-1}^{(r)}}^{-1} \cdots \tau_c^{-1} && \text{(by induction)} \\
&= x(1, m_{s-1}^{(r)}) \cdot \tau_{m_{s-1}^{(r)}}^{-1} \tau_{m_{s-1}^{(r)}+1}^{-1} \cdots \tau_c^{-1} && \text{(note that } x(1, m_{s-1}^{(r)}) = x(s-1, r)) \\
&= x(0, m_{s-1}^{(r)}) \cdot \tau_{m_{s-1}^{(r)}+1}^{-1} \cdots \tau_c^{-1} && \text{(note that } x(0, m_{s-1}^{(r)}) = x(s-2, r)) \\
&= \text{tr}|_{m_{s-1}^{(r)}, \ell}(y_\ell) \cdot \tau_{m_{s-1}^{(r)}+1}^{-1} \cdots \tau_c^{-1} && \text{(note that } x(0, m_{s-1}^{(r)}) = \text{tr}|_{m_{s-1}^{(r)}, \ell}(y_\ell)) \\
&= \text{tr}|_{m_{s-1}^{(r)}, \ell}(y_\ell),
\end{aligned}$$

as desired. We remark that the last equality in the previous computation follows from observing that $\text{tr}|_{m_{s-1}^{(r)}, \ell}(y_\ell)$ is not mutated in any of the mutation sequences $\underline{\mu}_{m_{s-1}^{(r)}+1}^{(r)}, \dots, \underline{\mu}_c$, and thus it is unaffected by any of the permutations $\tau_{m_{s-1}^{(r)}+1}^{-1}, \dots, \tau_c^{-1}$. By induction, this completes the proof. \square

8. ADDITIONAL QUESTIONS AND REMARKS

In this section, we give an example to show how our results provide explicit maximal green sequences for quivers that are not of type \mathbb{A} . We also discuss ideas we have for further research.

8.1. Maximal Green Sequences for Quivers Arising from Surface Triangulations. The following example shows how our formulas for maximal green sequences for type \mathbb{A} quivers can be used to give explicit formulas for maximal green sequences for quivers arising from other types of triangulated surfaces.

Example 8.1. Consider the marked surface (\mathbf{S}, \mathbf{M}) with the triangulation given as \mathbf{T} shown in Figure 36 on the left. The surface \mathbf{S} is a once-punctured pair of pants with triangulation

$$\mathbf{T} = \mathbf{T}_1 \sqcup \mathbf{T}_2 \sqcup \{\eta, \epsilon, \zeta\}$$

where $\alpha_1, \alpha_2, \alpha_3 \in \mathbf{T}_1$ and $\beta_1, \beta_2, \beta_3, \nu \in \mathbf{T}_2$. We assume that the boundary arcs b_i with $i \in [5]$ contain no marked points except for those shown in Figure 36. The other boundary arcs may contain any number of marked points. As in Section 4, let $Q_{\mathbf{T}}$ be the quiver determined by \mathbf{T} and let $v_\delta \in (Q)_0$ denote the vertex corresponding to arc $\delta \in \mathbf{T}$.

We can think of the marked surface $(\mathbf{S}_1, \mathbf{M}_1)$ determined by $c_1, \beta_1, b_1, c_2, \beta_2, b_2, \beta_3, b_3$ as an m_1 -gon where $m_1 = \#\mathbf{M}_1$ and we can think of \mathbf{T}_1 as a triangulation of \mathbf{S}_1 . Similarly, we can think of the marked surface $(\mathbf{S}_2, \mathbf{M}_2)$ determined by $\alpha_1, c_3, \eta, b_5, c_6, \alpha_3, c_5, b_2, \alpha_2, c_4, b_1$ as an m_2 -gon where $m_2 = \#\mathbf{M}_2$ and we can think of

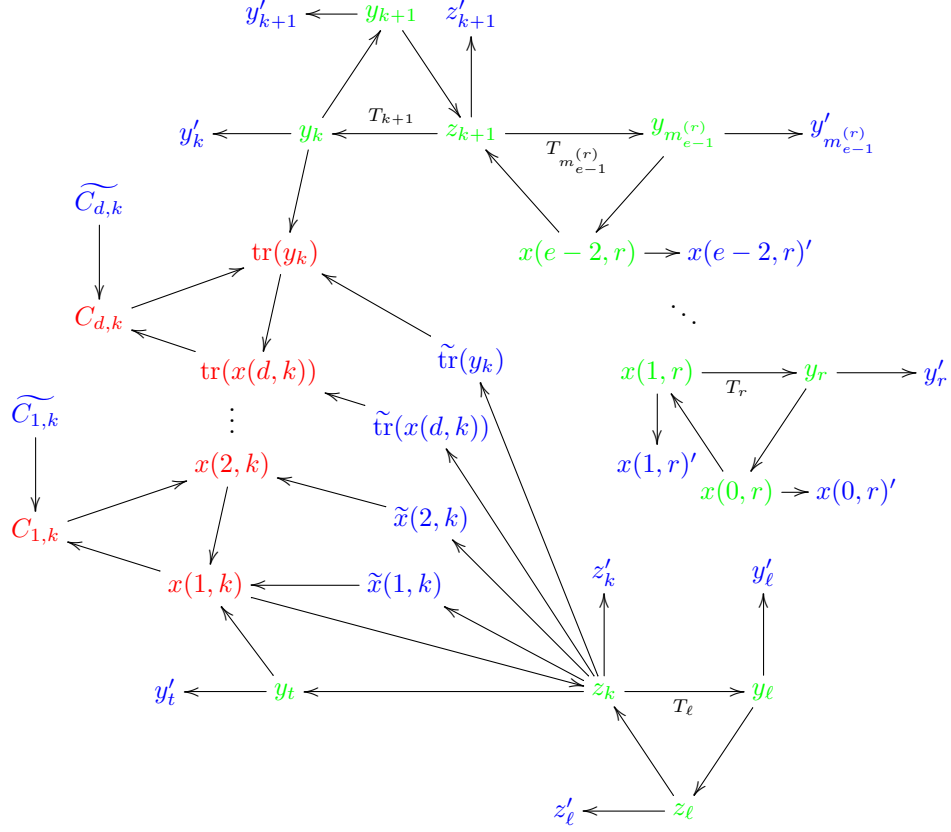


FIGURE 31. The full subquiver of $\underline{\mu}_{k-1} \circ \dots \circ \underline{\mu}_1 \circ \underline{\mu}_0(\widehat{Q})$ on the vertices and frozen vertices shown here.

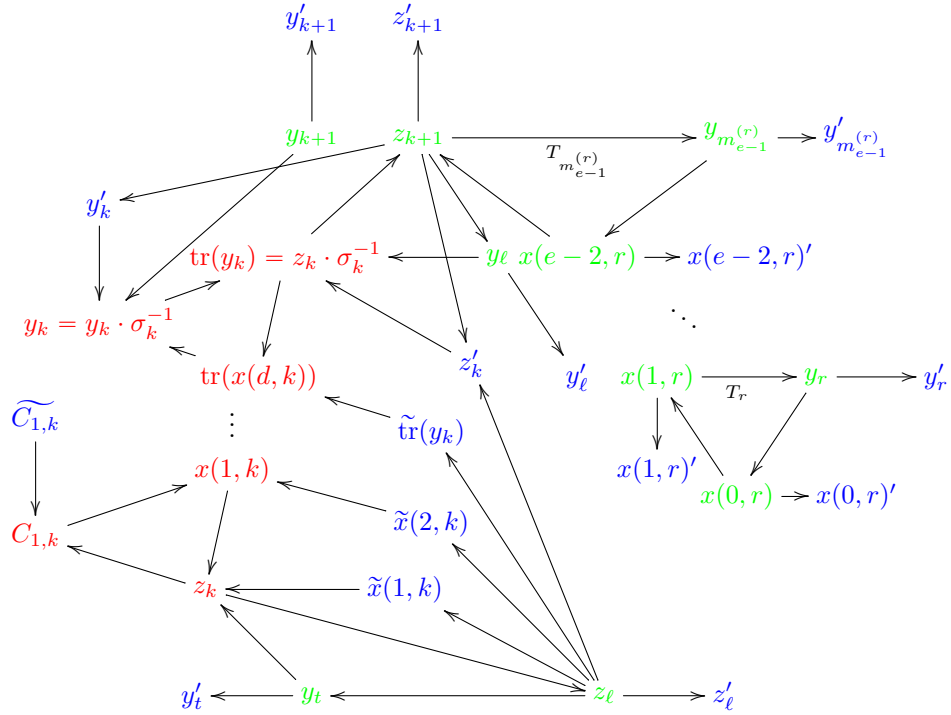


FIGURE 32. The full subquiver of $\underline{\mu}_k \circ \dots \circ \underline{\mu}_1 \circ \underline{\mu}_0(\widehat{Q})$ on the vertices and frozen vertices shown here.

30

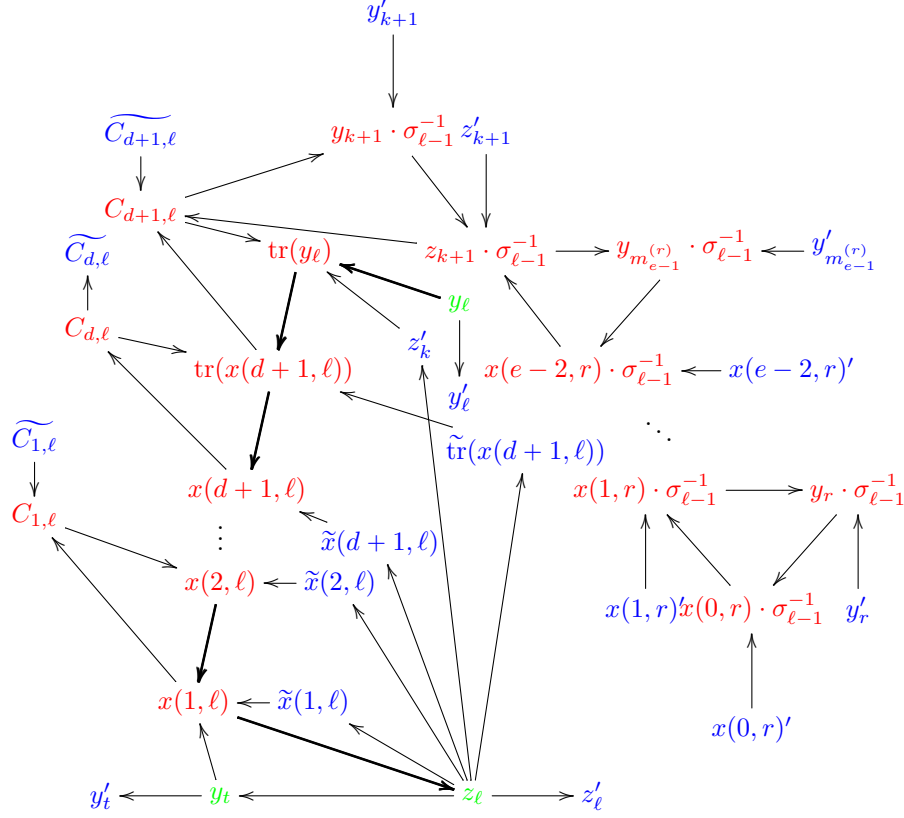


FIGURE 35. The effect of applying $\underline{\mu}_{\ell-1} \circ \dots \circ \underline{\mu}_{k+1}$ to $\underline{\mu}_k \circ \dots \circ \underline{\mu}_1 \circ \underline{\mu}_0(\hat{Q})$ where $C_{d+1, \ell} = y_k \cdot \sigma_{\ell-1}^{-1}$ and $\widetilde{C}_{d+1, \ell} = y'_k$, as desired. The mutation sequence $\underline{\mu}_\ell$ is indicated by the bold arrows.

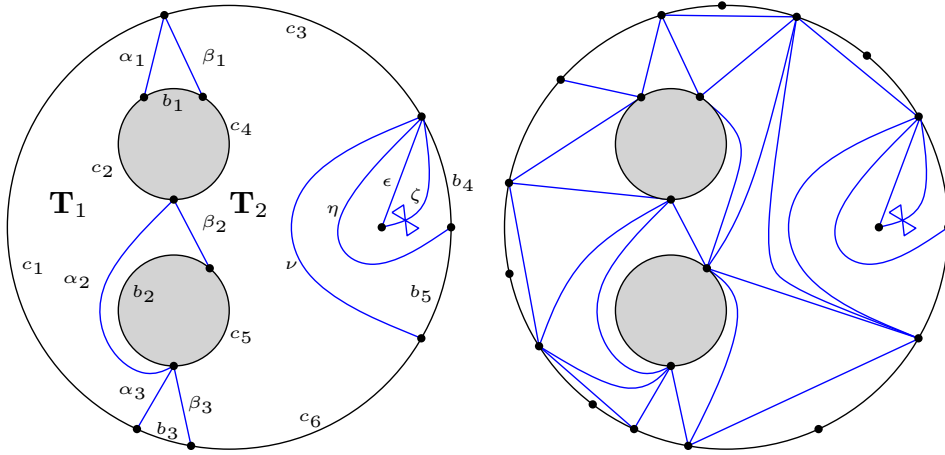


FIGURE 36.

Problem 8.2. Find explicit formulas for maximal green sequences for quivers arising from triangulations of surfaces.

Using Corollary 4.5, we can reduce Problem 8.2 to the problem of finding explicit formulas for maximal green sequences of irreducible quivers that arise from a triangulated surface. In [1], the authors sketch an argument showing the existence of maximal green sequences for quivers arising from triangulated surfaces. However, we

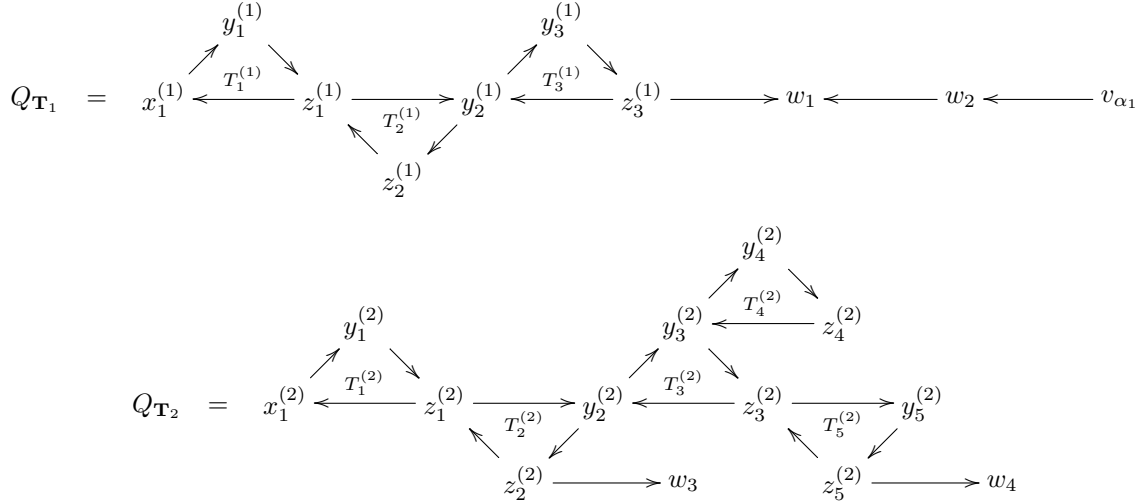


FIGURE 37.

would like to prove the existence of maximal green sequences by giving explicit formulas for maximal green sequences of such quivers.

Some progress has already been made in answering Problem 8.2. In [17], Ladkani shows that quivers arising from triangulations of once-punctured closed surfaces of genus $g \geq 1$ have no maximal green sequences. In [7, 8], explicit formulas for maximal green sequences are given for specific triangulations of closed genus $g \geq 1$ surfaces. In [9], a formula is given for the minimal length maximal green sequences of quivers defined by polygon triangulations. It would be interesting to understand, in general, what are the possible lengths that can be achieved by maximal green sequences of a given quiver.

8.2. Trees of Cycles. Our study of signed irreducible type \mathbb{A} quivers was made possible by the fact that such quivers are equivalent to labeled binary trees of 3-cycles (see Lemma 5.6). It is therefore reasonable to ask if one can find explicit formulas for maximal green sequences of quivers that are trees of cycles where each cycle has length at least $k \geq 3$. In our construction, we define a total ordering and a sign function on the set of 3-cycles of an irreducible type \mathbb{A} quiver (with at least one 3-cycle), and this data was important in discovering and describing the associated mutation sequence. One could use a similar technique to construct an analogue of the associated mutation sequence for quivers that are trees of oriented cycles.

Problem 8.3. Find a construction of maximal green sequences for quivers that are trees of oriented cycles.

8.3. Enumeration of Maximal Green Sequences. In the process of revising this paper, the problems posed in this section have been solved. For posterity, we keep this section as it appeared in the original `arXiv` version. A solution to Problem 8.4 appears in [12]. A solution to Problem 8.5 appears in [9].

For a given signed irreducible type \mathbb{A} quiver \mathcal{Q} with root 3-cycle T and with at least two 3-cycles our construction produces a maximal green sequence $\underline{\mu} = \underline{\mu}(T)$ of \mathcal{Q} for each leaf 3-cycle in \mathcal{Q} . It would be interesting to see how many maximal green sequences of \mathcal{Q} can be obtained from the maximal green sequences $\underline{\mu}$ as the choice of the root 3-cycle T varies.

Problem 8.4. Determine what maximal green sequences of \mathcal{Q} can be obtained via commutation relations and Pentagon Identity relations applied to the maximal green sequences in $\{\underline{\mu}(T) : T \text{ is a leaf 3-cycle}\}$.

Additionally, in [5] there are several tables giving the number of maximal green sequences of certain small rank quivers by length. These computations may be useful for making progress on the problem of enumerating maximal green sequences of quivers.

As discussed in Remark 6.6, the associated mutation sequences constructed here are not necessarily the shortest possible maximal green sequences. This motivates the following problem.

Problem 8.5. Provide a construction of the maximal green sequences of minimal length, possibly by showing how to apply Pentagon Identity relations to the associated mutation sequences.

8.4. Further Study of Maximal Green Sequences. Note that maximal green sequences of a quiver Q can be thought of as maximal chains (from the unique source to the unique sink) in the *oriented exchange graph* [5, Section 2]. In the case that Q is of type \mathbb{A} , the exchange graph is an orientation of the 1-skeleton of the associahedron. The oriented exchange graph is especially nice in the case when Q is a **Dynkin quiver** (i.e. an acyclic orientation of a Dynkin diagram of type \mathbb{A} , \mathbb{D} , or \mathbb{E}). For example, it is the Hasse graph of the Tamari lattice in the case Q is linear and equioriented and it is the Hasse graph of a Cambrian lattice (in the sense of Reading [20]) as is noted in [15, Section 3]. In particular, this means that we consider the finite Coxeter group G whose Dynkin Diagram is the unoriented version of Q and a choice of Coxeter element c compatible with the orientation of Q and then maximal green sequences are in bijection with maximal chains in the Cambrian lattice, a quotient of the weak Bruhat order on G . Note, that this bijection is studied further in [19] where each c -sortable word is shown to correspond to a green sequence.

To indicate the difficulty of describing the set of maximal green sequences once we consider quivers with cycles, we focus on the A_3 case here. In the case where Q is a 3-cycle (with $1 \rightarrow 2, 2 \rightarrow 3, 3 \rightarrow 1$), there is not a corresponding Cambrian congruence that one can apply to the weak Bruhat order on the symmetric group $G = S_4$ to obtain the desired Hasse diagram. In particular, the corresponding Cambrian lattice is constructed from the geometry of the affine \tilde{A}_2 root system instead of from a finite Coxeter group. Intersecting this coarsening of the Coxeter Lattice with the Tits Cone yields 11 regions rather than the 14 we obtain in the acyclic case [21].

Nonetheless, we can still compute maximal green sequences in this case, and see that they are indeed the set of oriented paths through a certain orientation of the 1-skeleton of the associahedron. There are six possible maximal green sequences of length 4: $\mu_1 \circ \mu_3 \circ \mu_2 \circ \mu_1$, $\mu_2 \circ \mu_1 \circ \mu_3 \circ \mu_2$, $\mu_3 \circ \mu_2 \circ \mu_1 \circ \mu_3$, $\mu_3 \circ \mu_1 \circ \mu_2 \circ \mu_1$, $\mu_1 \circ \mu_2 \circ \mu_3 \circ \mu_2$, and $\mu_3 \circ \mu_2 \circ \mu_1 \circ \mu_3$. We can find three more maximal green sequences of length 5: $\mu_2 \circ \mu_3 \circ \mu_2 \circ \mu_1 \circ \mu_2$, $\mu_3 \circ \mu_1 \circ \mu_3 \circ \mu_2 \circ \mu_3$, and $\mu_1 \circ \mu_2 \circ \mu_1 \circ \mu_3 \circ \mu_1$. As in Figure 22 of [5], there are no other maximal green sequences of this quiver. To obtain these sequences of length 5, we select any of the first three maximal green sequences of length 4. We then apply the relation $\mu_{i+1} \circ \mu_i \sim \mu_{i+1} \circ \mu_i \circ \mu_{i+1}$ (where the arithmetic is carried out mod 3) and apply the vertex permutation $(i, i+1)$ to the vertices at which one mutates later in the sequence.

In an attempt to understand this example in terms of the Coxeter group of type A_3 , i.e. S_4 , we consider the presentation described in [4] for quivers with cycles. In this case, if we let $s_1 = (14)$, $s_2 = (24)$, $s_3 = (34)$, we obtain

$$S_4 = \langle s_1, s_2, s_3 : s_1^2 = s_2^2 = s_3^2 = (s_1 s_2)^3 = (s_2 s_3)^3 = (s_3 s_1)^3 = (s_1 s_2 s_3 s_2)^2 = 1 \rangle.$$

Unlike the acyclic A_3 case where the permutation in S_4 corresponding to the longest word, i.e. 4321, is the only element of S_4 whose length as a reduced expression, e.g. $s_1 s_2 s_3 s_1 s_2 s_3$, is of length 6, in the Barot-Marsh presentation, the permutations 4321, 3412, 2143, 1342, and 1432 all have reduced expressions of maximal length, namely 4.

Further, if we visualize the order complex of S_4 under this presentation, we obtain a torus (see Example 3.1 of [3]) rather than a simply-connected surface like the acyclic case and there are no permutations with reduced expression of length 5, hence reduced expressions in this presentation cannot correspond to maximal green sequences. We thank Vic Reiner for bringing his paper with Eric Babson to our attention. Hence, understanding the full collection of maximal green sequences for other quivers with cycles, even those of type \mathbb{A} , appears to require more than an understanding of the associated Coxeter groups.

Since our original preprint, in recent work [12] (resp. [13]) of the first author and Thomas McConville, an analogue of the weak order on S_n , known as the lattice of **biclosed subcategories** (resp. **biclosed sets of segments**) is constructed. In [12] and [13], it is shown that the oriented exchange graph of quivers of type \mathbb{A} can be obtained as a lattice quotient of these. This lattice congruence generalizes the Cambrian congruence in type \mathbb{A} . Additionally, the results in [12] and [13] do require techniques from representation theory of finite dimensional algebras, which further suggests that understanding the full collection of maximal green sequences for quivers with cycles may require more than elementary techniques.

REFERENCES

- [1] M. Alim, S. Cecotti, C. Córdova, S. Espahbodi, A. Rastogi, and C. Vafa. BPS quivers and spectra of complete $\mathcal{N} = 2$ quantum field theories. *Communications in Mathematical Physics*, 323(3):1185–1227, 2013.
- [2] C. Amiot. Cluster categories for algebras of global dimension 2 and quivers with potential. In *Annales de l'institut Fourier*, volume 59, pages 2525–2590. Association des Annales de l'institut Fourier, 2009.
- [3] E. Babson and V. Reiner. Coxeter-like complexes. *Discrete Mathematics & Theoretical Computer Science*, 6(2):223–252, 2004.
- [4] M. Barot and R. Marsh. Reflection group presentations arising from cluster algebras. *Transactions of the American Mathematical Society*, 367(3):1945–1967, 2015.

- [5] T. Brüstle, G. Dupont, and M. Pérotin. On maximal green sequences. *International Mathematics Research Notices*, 2014(16):4547–4586, 2014.
- [6] A. B. Buan and D. F. Vatne. Derived equivalence classification for cluster-tilted algebras of type A_n . *J. Algebra*, 319(7):2723–2738, 2008.
- [7] E. Bucher. Maximal green sequences for cluster algebras associated to the n -torus. *arXiv preprint arXiv:1412.3713*, 2014.
- [8] E. Bucher and M. R. Mills. Maximal green sequences for cluster algebras associated to the orientable surfaces of genus n with arbitrary punctures. *arXiv preprint arXiv:1503.06207*, 2015.
- [9] E. Cormier, P. Dillery, J. Resh, K. Serhiyenko, and J. Whelan. Minimal length maximal green sequences and triangulations of polygons. *arXiv preprint arXiv:1508.02954*, 2015.
- [10] H. Derksen, J. Weyman, and A. Zelevinsky. Quivers with potentials and their representations II: applications to cluster algebras. *J. Amer. Math. Soc.*, 23(3):749–790, 2010.
- [11] S. Fomin, M. Shapiro, and D. Thurston. Cluster algebras and triangulated surfaces. part I: Cluster complexes. *Acta Mathematica*, 201(1):83–146, 2008.
- [12] A. Garver and T. McConville. Lattice properties of oriented exchange graphs and torsion classes. *arXiv preprint arXiv:1507.04268*, 2015.
- [13] A. Garver and T. McConville. Oriented flip graphs and noncrossing tree partitions. *arXiv preprint arXiv:1604.06009*, 2016.
- [14] B. Keller. On cluster theory and quantum dilogarithm identities. In *Representations of Algebras and Related Topics*, Editors A. Skowronski and K. Yamagata, *EMS Series of Congress Reports*, European Mathematical Society, pages 85–11, 2011.
- [15] B. Keller. Quiver mutation and combinatorial DT-invariants. FPSAC 2013 Abstract, 2013.
- [16] M. Kontsevich and Y. Soibelman. Motivic donaldson-thomas invariants and cluster transformation. *arXiv preprint arXiv:0811.2435*, 2008.
- [17] S. Ladkani. On cluster algebras from once punctured closed surfaces. *arXiv preprint arXiv:1310.4454*, 2013.
- [18] G. Muller. The existence of a maximal green sequence is not invariant under quiver mutation. *arXiv preprint arXiv:1503.04675*, 2015.
- [19] Y. Qiu. C-sortable words as green mutation sequences. *Proceedings of the London Mathematical Society*, 111(5):1052–1070, 2015.
- [20] N. Reading. Cambrian lattices. *Advances in Mathematics*, 2(205):313–353, 2006.
- [21] N. Reading and Speyer D. personal communication.
- [22] A. I. Seven. Maximal green sequences of exceptional finite mutation type quivers. *Symmetry, Integrability and Geometry. Methods and Applications*, 10, 2014.